

A Pilot Study on the Design of Multiple Debris-resisting Barriers

GEO Report No. 319

J.S.H. Kwan, R.C.H. Koo & F.W.Y. Ko

**Geotechnical Engineering Office
Civil Engineering and Development Department
The Government of the Hong Kong
Special Administrative Region**

A Pilot Study on the Design of Multiple Debris-resisting Barriers

GEO Report No. 319

J.S.H. Kwan, R.C.H. Koo & F.W.Y. Ko

**This report was originally produced in October 2013
as GEO Technical Note No. TN 3/2013**

© The Government of the Hong Kong Special Administrative Region

First published, June 2016

Prepared by:

Geotechnical Engineering Office,
Civil Engineering and Development Department,
Civil Engineering and Development Building,
101 Princess Margaret Road,
Homantin, Kowloon,
Hong Kong.

Preface

In keeping with our policy of releasing information which may be of general interest to the geotechnical profession and the public, we make available selected internal reports in a series of publications termed the GEO Report series. The GEO Reports can be downloaded from the website of the Civil Engineering and Development Department (<http://www.cedd.gov.hk>) on the Internet. Printed copies are also available for some GEO Reports. For printed copies, a charge is made to cover the cost of printing.

The Geotechnical Engineering Office also produces documents specifically for publication in print. These include guidance documents and results of comprehensive reviews. They can also be downloaded from the above website.

The publications and the printed GEO Reports may be obtained from the Government's Information Services Department. Information on how to purchase these documents is given on the second last page of this report.



H.N. Wong
Head, Geotechnical Engineering Office
June 2016

Foreword

This report presents a pilot study on the design of multiple debris-resisting barriers for mitigating natural terrain landslide hazards. It reviews the available literature and overseas design practices on the subject. A suggested framework and pertinent factors to be considered in the design are proposed.

The work was carried out by a working group comprising Dr J.S.H. Kwan, Mr R.C.H. Koo, Ms F.W.Y. Ko, Mr F.L.C. Lo, Mr T.L. Yeung and Ms I.C.Y. Yu. Mr T.H. Lo, under the supervision of Mr R.C.H. Koo, carried out a Particle Image Velocimetry analysis on the image records of the flume tests performed by the Hong Kong University of Science and Technology. The working group was initially steered by Mr Ken K.S. Ho and by me at a later stage.

Draft version of the report was reviewed by Professor P. Cui of the Institute of Mountain Hazards and Environment, China and Professor O. Hungr of the University of British Columbia, Canada. Practitioners of the industry, including Mr Malcom Lorimer of Jacobs China Ltd., Mr Stuart Millis of Arup, Hong Kong and Mr Chris Lee of C M Wong & Associates Ltd. provided insightful comments on the draft version of the report. Many colleagues in the office also provided useful comments on the report. All contributions are gratefully acknowledged.



Y.K. Shiu

Chief Geotechnical Engineer/Standards & Testing

Abstract

Overseas experience suggests that multiple barriers can potentially be a practicable alternative means to mitigate reasonably large debris avalanches and debris flows. Possibly, multiple barriers could provide a viable solution to mitigate, for example, low-frequency, large magnitude events in catchments with major drainage lines in Hong Kong. A pilot study on the design of multiple debris-resisting barriers for mitigating natural terrain landslide hazards in channelised debris flow catchments and topographic depression catchments has been conducted.

This report documents the pilot study which reviews the available literature and overseas design practices on the subject, and suggests a preliminary design framework involving the use of ‘staged mobility analysis’. Two worked examples are included in this report for illustration purposes.

The suggested design framework is not mandatory. Practitioners may choose other appropriate design methodology for their multiple barrier designs. Key technical factors to be considered in the design of multiple barriers are also suggested.

Contents

	Page No.
Title Page	1
Preface	3
Foreword	4
Abstract	5
Contents	6
List of Tables	8
List of Figures	9
1 Introduction	10
1.1 Background	10
1.2 Study Scope	10
2 Design and Use of Multiple Barriers in Practice	11
2.1 Retention Capacity	11
2.2 Minimum Spacing of Barriers Debris	13
2.3 Trajectory and Impact Velocity	13
3 Suggested Design Framework	16
3.1 Key Parameters for Design of Multiple Barriers	16
3.2 Design Scenario	17
3.3 Retention Capacity	19
3.4 Debris Mobility Analysis	19
3.5 Barrier Location	23
4 Other Design Considerations	24
4.1 Intermediate and Terminal	24
4.2 Barriers Drainage Provisions	24
4.3 Downstream Scouring	25
4.4 Detailing	26
5 Illustrative Examples	27

	Page No.
6 Discussion	27
6.1 Suggestions on Further Work	29
7 Conclusions	29
8 References	29
Appendix A: Flume Tests by the Hong Kong University of Science and Technology	33
Appendix B: Illustrative Examples	41

List of Tables

Table No.		Page No.
3.1	Suggested Values of C_x	22

List of Figures

Figure No.		Page No.
2.1	Debris Deposition Profile and Minimum Spacing of Barriers	12
2.2	Debris Overflows from Crest of Rigid Barrier	14
2.3	Left: Rock Blocks Used in the Flume Tests by Yang et al (2011); Right: Flume Test Involving Ballistic Flight of Rock Blocks	15
3.1	Design Scenario	18
3.2	Location of Landslide Source for Design of Different Rows of Barrier	18
3.3	Design Parameters for Assessing Dynamic Motion of Landslide Debris Overflowing from a Barrier	20
3.4	A Case where the Length of Debris is Longer than the Length of Debris Trajectory	23
4.1	Lattice Structure and Flexible Barrier	24
4.2	Detailing of Barriers	26

1 Introduction

1.1 Background

Multiple debris-resisting barriers (hereinafter referred to as multiple barriers) have been adopted in many overseas countries to mitigate landslide hazards, such as debris avalanches and debris flows. In general, multiple barriers comprise rows of single barrier installed at different strategic positions along the runout path(s) of a given debris avalanche or debris flow. Each of these rows of single barrier is designed to retain a portion of the failure volume. Because of this, the scale of the individual barrier, in terms of structural requirements and retaining height, could be optimized to cope with the site constraints and may prove to be more effective in minimizing entrainment. This could enhance the buildability of barriers and facilitate the use of smaller scale debris-resisting barriers. Overseas experience suggests that multiple barriers can potentially be a practicable alternative means to mitigate reasonably large debris avalanches and debris flows, possibly including low-frequency, large magnitude events in catchments with major drainage lines, in Hong Kong.

There are so far no well-established international or local design guidelines for multiple barriers. This has hindered the development and application of multiple barriers in Hong Kong. For possible advancement of the use of multiple barriers for mitigation of debris flows in channelized catchments and topographical depression catchments, it is considered useful to formulate a preliminary design methodology for practitioners' trial use. Draft version of the report was reviewed by Professor P. Cui of the Institute of Mountain Hazards and Environment, China and Professor O. Hungr of the University of British Columbia, Canada.

1.2 Study Scope

In this Technical Note, multiple barriers are taken to be non-sacrificial barriers, and they serve to retain landslide debris (see definitions of non-sacrificial barriers in Kwan & Cheung, 2012). Design of sacrificial barriers that aim to dissipate kinetic energy of landslide debris without debris storage function is not covered in this Technical Note.

The primary objective of the pilot study is to formulate a preliminary framework for design of multiple barriers using force approach (Kwan, 2012; Kwan & Cheung, 2012) for topographic depression (TD) catchments and channelised (CD) catchments (see GEO (2013) for the definitions TD and CD catchments). The proposed preliminary design framework should not be regarded as a mandatory standard for multiple barrier design. Designers may choose other appropriate design methodology for their multiple barrier designs. Detailed structural design of multiple barriers is not covered in this study. The present study comprises the following key tasks:

- (a) review of international practice on the design and use of multiple barriers in mitigating natural terrain landslide hazards;
- (b) formulation of a preliminary design framework for multiple barriers;

- (c) suggestion of good practice in relation to other key design considerations; and
- (d) recommendations on further development work.

2 Design and Use of Multiple Barriers in Practice

Multiple barriers have been used to mitigate landslide hazards from debris avalanches and debris flows in many places, such as Switzerland, Japan, Mainland China and Taiwan (Shum & Lam, 2011). Although a comprehensive set of design guidelines for multiple barriers is not available in international or national standards, various international publications give guidance and recommend good practice on certain design aspects of multiple barriers. For examples, CGS (2004) and NILIM (2007) provide guidelines for calculating retention volume of barriers, SWCB (2005) recommends the minimum spacing between barriers, and Wendeler et al (2012) document a case study of designing a multiple barrier scheme in Switzerland. Wong (2009) suggested that building a series of barriers along the drainage line may prove to be more effective in minimising entrainment and overcoming site constraints. Salient points and details of the available design guidance and prevailing practice are summarised in the following sections.

2.1 Retention Capacity

The total retention capacity of multiple barriers is taken as the sum of the retention capacity of each individual barrier (Wendeler, 2010; Zhou et al, 1991). The retention capacity of a barrier can be established based on the overall geometry of barriers, ground profile and angle of debris deposition.

CGS (2004) recommended that in establishing the retention capacity of a rigid barrier, the angle of debris deposition can be assumed to be 1/2 to 3/4 of that of the ground profile (Figure 2.1). Design guidance used in other areas, such as SWCB (2005) of Taiwan and NILIM (2007) of Japan, recommended a relatively smaller debris deposition angle.

NILIM (2007), based on field observations in Japan, recommended that the maximum angle of debris deposition could be half of that of the ground profile. This angle could be reduced to 1/6 of the inclination of the runout profile if drift woods are present in debris flow. SWCB (2005) suggested the same upper bound angle, the lower bound angle adopted in the practice of Taiwan is 1/3 of that of the ground profile (see Figure 2.1).

A relationship between debris deposition angle and debris retention volume was reported by VanDine (1996), which showed that the debris deposition angle could be as low as 6° for debris retention volume not exceeding $20,000 \text{ m}^3$.

Osti et al (2007) carried out a series of small scale laboratory flume tests and suggested that the inclination of the debris deposition profile could be correlated with the angle of shearing resistance (θ_s) of the debris and sediment concentration of the debris flow. If the debris flow is fully saturated with sediments, the angle of debris deposition would be taken as $1/2 \tan \theta_s$. The value of θ_s could be close to the friction angle that controls the basal

resistance of the debris flow. Adopting the concept of equivalent friction angle as mentioned by Kwan & Cheung (2012), the equivalent friction angle which governs the basal resistance relates to the rheological parameters adopted in debris mobility analysis. In local practice, the equivalent friction angle generally assumed ranges from approximately 20° to 30°. It follows that the angle of debris deposition could be in the range of 10° to 16°. This range is consistent with the results of the flume tests reported by Lin et al (2007), who observed that debris deposition angles ranged between 9° and 21°.

The above summarises the debris deposition angles behind rigid barriers. Geobruigg (2012) conducted a review of the retention capacity of flexible debris-resisting barriers. Based on their field observations and experience, they recommended that calculations of the design retention capacity of a flexible debris-resisting barrier should take account of the reduced height of the barrier and should ignore the volume in the bugled-out portion of the barrier. In addition, Geobruigg proposed that the angle of debris deposition behind the flexible barrier should be assumed to be horizontal.

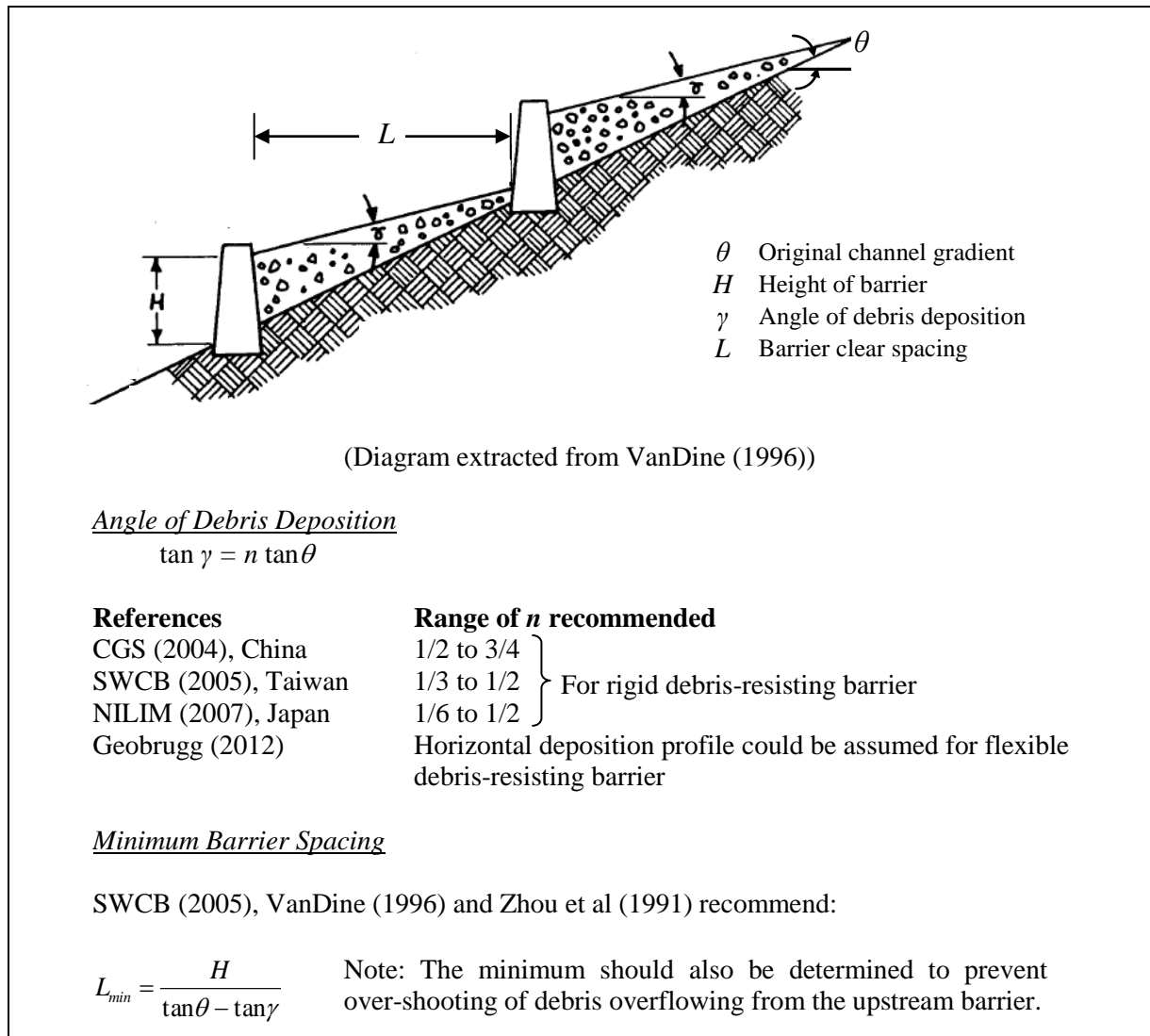


Figure 2.1 Debris Deposition Profile and Minimum Spacing of Barriers

2.2 Minimum Spacing of Barriers

The requirement for the minimum spacing between multiple barriers is promulgated in a number of design guidelines and literatures. Volkwein et al (2011) noted that hydraulic jump and back-waves could result when the debris flow is intercepted by barriers. The back-waves that propagate upstream could adversely affect the preceding barrier (e.g. in terms of scouring). Thus, a sufficiently large spacing between barriers should be specified. The recommendation on the minimum spacing between barriers by Zhou et al (1991), VanDine (1996) and SWCB (2005) is shown in Figure 2.1. According to SWCB (2005), the recommendation is aimed to prevent the adverse effects of back-waves.

The minimum spacing should take into account the debris trajectory from the upper barrier, which should not shoot over the downstream barrier, and should avoid the adverse effects of back-waves on the preceding barriers. However, when the adverse effects of back-waves on the preceding barriers are considered not relevant (e.g. floor of the runout path is not erodible or adequate erosion protections against the actions of back-wave are provided), the minimum spacing can be determined with the consideration of over-shooting only. For flexible barrier, the deformation of barrier should be also considered for the minimum clear spacing between barriers.

2.3 Debris Trajectory and Impact Velocity

Cui (2012) cautioned that the overflow velocity may be potentially affected by the geometry of the overflow weir and debris flow dynamic properties, based on the field observations in Mainland China. However, according to Cui (op cit), rigorous assessment of the effect of the geometry is not available at the moment. Speerli et al (2010) reported several debris flow flume tests to examine the dynamics of debris overflowing from small-scale ring-net barriers. A mixture of clayey gravelly sand and water was used in their tests. They observed that debris followed a projectile path after overtopping from the barrier and the debris was retarded upon impacting on the flume bed at the landing position. However, the corresponding velocity reduction was not reported.

The GEO has recently commissioned the Hong Kong University of Science and Technology (HKUST) to conduct flume tests to investigate the dynamics of debris overflowing from vertical rigid barriers. Dry sand was used in this series of flume tests. Photographic records of the tests showed that debris, after hitting and filling up the rigid barrier, launched into a ballistic flight from the crest of the barrier and resumed its travel on the flume bed upon landing. Efforts have been made to quantify the velocity reduction at landing by interpreting the results of the flume tests using the Particle Image Velocimetry (PIV) technique developed by White et al (2003).

Typical results produced by the PIV package PIV are presented in Figure 2.2. This shows the velocity at the instant of about 0.5 second after the sand impacted on the barrier. The sand overflowed from the crest of the barrier at a velocity of about 1 m/s and launched into a ballistic flight. It followed a projectile trajectory and finally landed on the flume bed at a maximum distance of 0.21 m downstream of the barrier. Due to the gain in potential energy, the sand flow accelerated along the trajectory path. The maximum velocity was up to about 1.8 m/s immediately before landing. Upon landing, the sand flow travelled along

the flume bed without any noticeable rebound. In addition, the sand flow velocity was reduced after landing. The ratio of the velocity parallel to the flume after and before impact has been determined at various times during the test. This velocity ratio ranged from about 0.3 to 0.5. It should be noted that dry sand is ideally frictional and develops high flow resistance at the impact point, where the normal momentum of the falling mass creates a large normal force. In case of saturated materials in the field, however, such an impact may create high pore-pressure in the debris, resulting in the effective normal stress and hence flow resistance at a lower value. A control test had been carried out as a benchmark to the debris frontal velocity without barrier. Appendix A presents details of the test set-up and interpretation of test results.

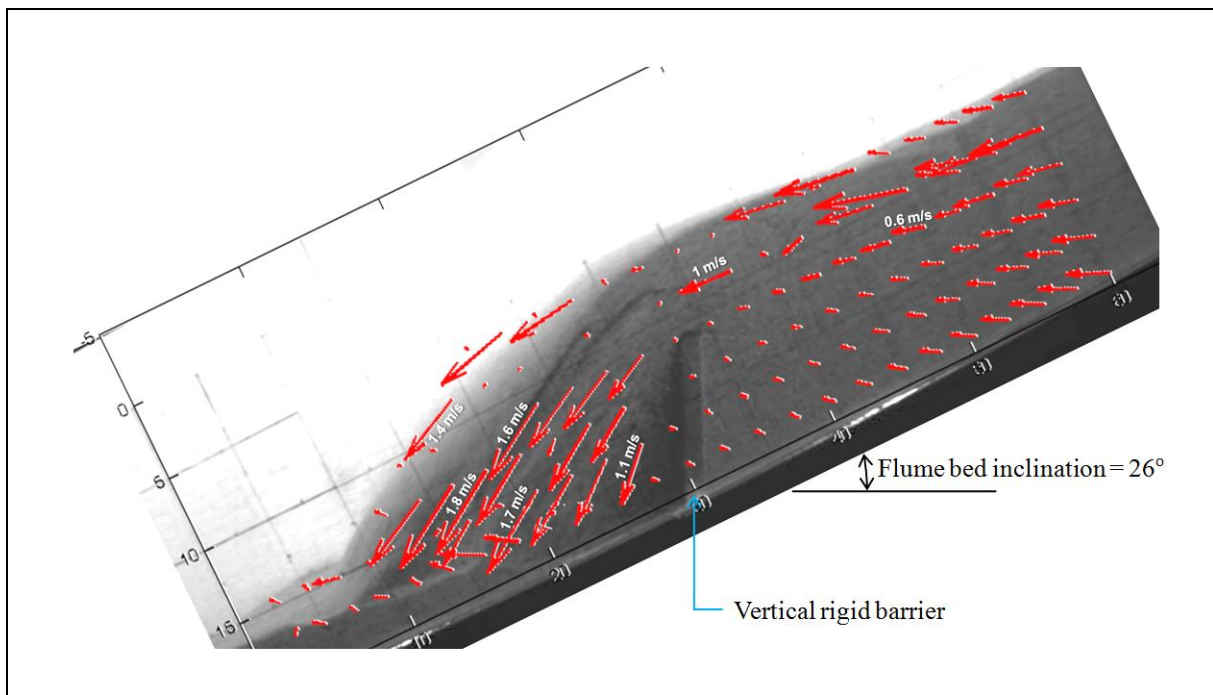


Figure 2.2 Debris Overflows from Crest of Rigid Barrier

Flume tests involving ballistic trajectory of dry granular flow comprising rock blocks had been conducted by Yang et al (2011) (see Figure 2.3). The rock blocks used in their experiments were of dimension of up to 0.1 m. According to Yang et al (op cit), the granular flows in their tests involved rolling and bouncing of large granular particles. These flume tests may replicate the dynamics of debris avalanche. They observed that the granular flow was subjected to velocity reduction upon landing on the flume bed. Yang et al (2012) reported that the velocity reduction ratio immediately after and before landing ranged from 0.41 to 0.75 with an average of 0.65.



Figure 2.3 Left: Rock Blocks Used in the Flume Tests by Yang et al (2011); Right: Flume Test Involving Ballistic Flight of Rock Blocks

Head loss of debris flows dropping from height has been studied by Chen et al (2009). They carried out measurements along debris transport channels equipped with drop structures, and suggested a formula for estimation of head loss of debris flow dropping from height. The velocity of the debris flows reported by Chen et al (op cit) ranged from 3 m/s to 6 m/s and the debris transport channels under their study were gently inclined (about 10°). Based on the suggested formula, it can be estimated that the ratio of velocity in the direction of the downstream channel after and before landing is in the order of 0.3 for debris flow of thickness ranging from 0.5 m to 1.5 m with a drop height of 2 m to 4 m.

In Hong Kong, it is common practice to estimate the impact velocity at a barrier using numerical mobility analyses such as DAN-W (Hung, 1995) or 2d-DMM (Kwan & Sun, 2006). 2d-DMM is currently not equipped with the capacity to simulate the dynamics of debris overflow from barriers. However, DAN-W is equipped with a module for modeling 'projectile flight'. In addition, DAN-W was used to simulate the progress of debris filling up behind a barrier (Mancarella & Hung, 2010), from which the deposition or storage angle of the debris surface can be assessed.

Some of the numerical models developed based on flood routing formulations are capable of simulating the hydraulics of debris flow along a path with multiple barriers, e.g. the computer program, Kanako 2D. According to Nakatani et al (2008), the program solves the modified shallow water equations with consideration of sediment concentration in the calculation of mass balance. The volume of deposition behind a barrier is calculated based on an empirical relationship between particle size of sediment and sediment concentration. Numerical integration of the governing equations is carried out over an Eulerian grid in a

depth-average manner. Input parameters including hydrograph of debris flow height at source, Manning's coefficient of runout path, geometry of debris trail, and initial sediment concentration of debris flow are required, in contrast with the current local practice. Wendeler et al (2012) reported a multiple barrier design in Switzerland to mitigate a channelized debris flow with a total volume of 15,000 m³. They estimated the debris velocity based on the largest super-elevation observed on site and adopted this debris velocity as the design impact velocity for design of all barriers in the multiple barrier system. No debris mobility analysis was performed.

3 Suggested Design Framework

3.1 Key Parameters for Design of Multiple Barriers

The use of multiple barriers provides a possible option of natural terrain hazard mitigation measure in Hong Kong. A suggested design framework is presented in the following but it should be noted that designers may adopt other design methodology as deemed appropriate and within suitable justifications. Having reviewed the international practice on the design and use of multiple barriers to resist or retain landslide debris from debris avalanches and debris flows, the following key parameters are considered crucial to the design of multiple barriers:

- (a) Design scenario - This is concerned with the determination of design events for the design of multiple barriers within a hillside catchment. Several design volumes for each landslide hazard within a hillside catchment are needed to reflect different probable scales of failure at different portions of a hillside catchment.
- (b) Retention capacity - This relates to an optimum combination of landslide volumes that can be retained behind multiple barriers in order to mitigate landslide hazards effectively. The retention capacity of a barrier depends on the overall geometry of the barrier, terrain gradient and debris deposition profile behind the barrier.
- (c) Debris trajectory and impact velocity - This is concerned with the dynamics of debris overflow from multiple barriers and the subsequent changes in debris velocity. When a given landslide impacts on a barrier, its runout profile is modified as the landslide debris gradually fills up the space behind the barrier. A portion of the landslide debris is trapped and retained by the barrier while the remaining landslide debris launches into a ballistic flight path and continues to cascade down the runout path after landing. The dynamics of this process involve acceleration during the ballistic flight and velocity reduction upon landing. The changes in debris velocity throughout this process at each barrier should be considered in order to realistically

simulate the debris movement at the downstream area.

- (d) Barrier location and other considerations - Multiple barriers should be placed at strategic locations such that landslide hazards are mitigated efficiently and effectively. Retention capacity, debris deposition angle and length of downstream scouring are some of the crucial factors that need to be considered. The possibility of debris overshooting to adjacent hillsides, and locations of steep gradient and soft ground are other key issues that should be taken into account. For the use of flexible debris-resisting barriers, the deformation and reduced height of flexible barriers due to debris impact should be duly incorporated in the design consideration. In addition, the use of secondary mesh in the intermediate flexible barriers to enhance the protection against the passage of fines reaching the downstream facilities should also be considered.

3.2 Design Scenario

Multiple barriers comprise rows of single barrier installed at different elevations of a hillside. Each of these rows should be designed with due consideration of the following scenarios:

- (a) barrier to resist impact by landslide debris overflowing from the preceding one (see Figure 3.1(a)); and
- (b) barrier to resist impact by debris from a slope failure on the hillside portion below the preceding one (see Figure 3.1(b)).

Figure 3.2 illustrates the overall concept of the above.

In current design practice, the design volumes for failures in channelized catchments or topographical depression catchments are established as appropriate during the natural terrain hazard study. A single design volume for each type of landslide hazard is usually sufficient for the design of mitigation measures near the toe of the hillside catchment.

As illustrated in Figure 3.2, possible landslide at different portions of a hillside should be considered for the design of different rows of barrier. For a given hillside catchment, the idea of using multiple barriers should be planned at an early stage of the natural terrain hazard study as far as possible so that the required design scenarios are duly established by the study. If the use of multiple barriers is only considered in the detailed design stage of natural terrain hazard mitigation measures, it may be necessary to re-assess the hillside hazards in order to determine the design volumes for different portions of the hillside catchment.

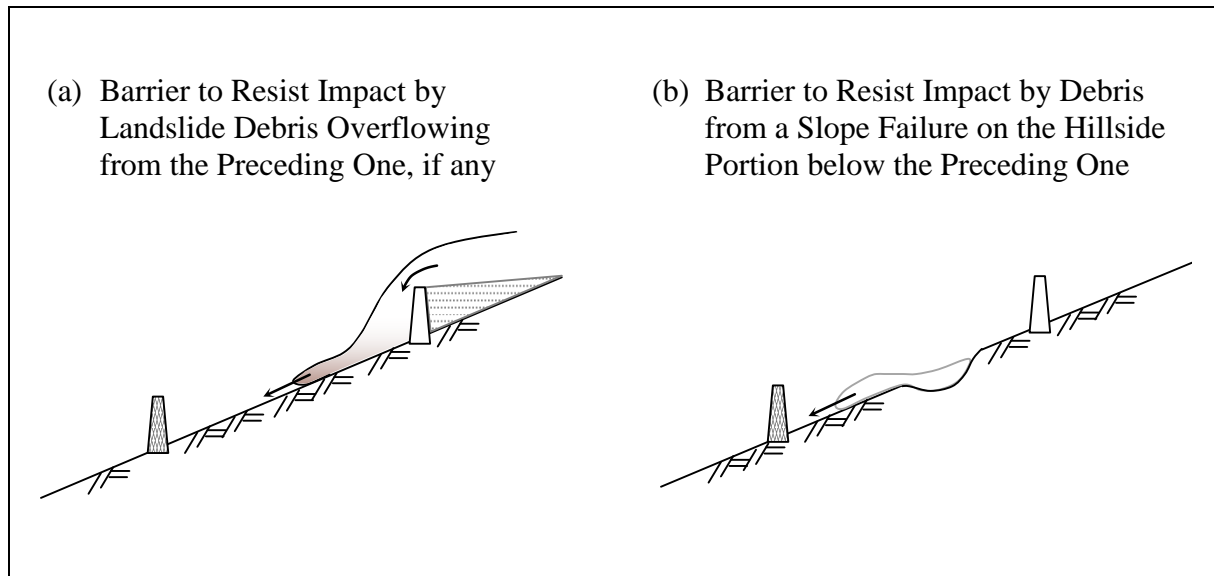


Figure 3.1 Design Scenario

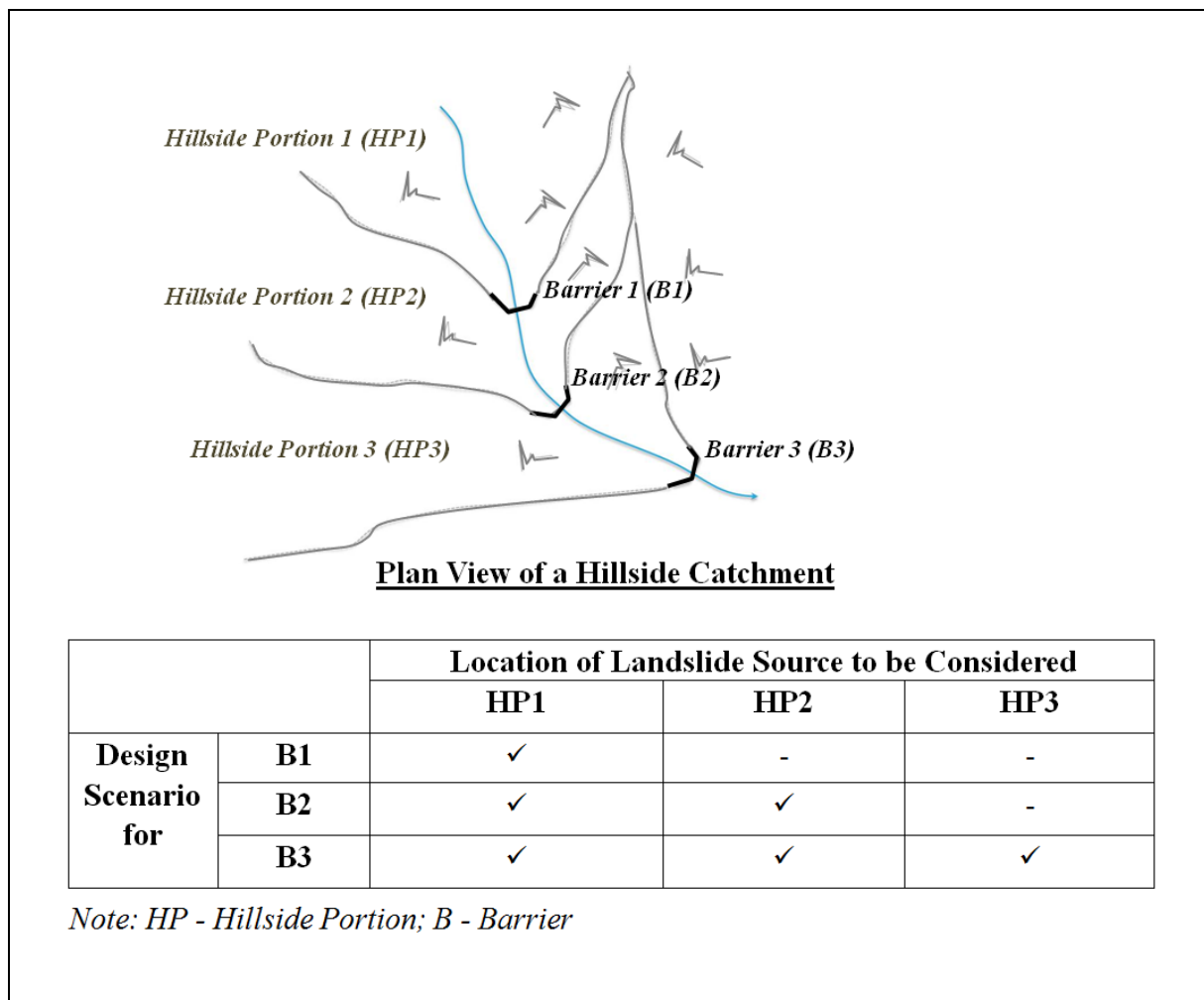


Figure 3.2 Location of Landslide Source for Design of Different Rows of Barrier

Attention should be given to the design retention capacity of multiple barriers (i.e. the sum of retention capacity of all barriers, including intermediate and terminal barriers). Figure 3.2 illustrates the design landslide scenarios that need to be considered.

3.3 Retention Capacity

The amount of landslide debris that can be retained behind a barrier depends on the geometry of debris retention zone and debris deposition profile. Based on the research by Osti et al (2007) and the concept of equivalent friction angle, the angle of debris deposition behind rigid barriers could range from 10° to 16° (see Section 2.1). For flexible barriers, Wendeler (2008) suggested that the angle of debris deposition should be $2/3$ of the average of slope gradient for flexible debris-resisting barrier. Geobruigg (2012) recommended to adopt a horizontal deposition profile and to use reduced net height (equal to $3/4$ of the original height of flexible barrier) after the debris impact for flexible debris-resisting barrier. Also, they suggested that the volume in the deformed bulge of the net should be ignored in the design. It is suggested that designers should follow the specific recommendations of the relevant manufacturers with due consideration of the site-specific conditions in order to determine the design retention capacity of flexible barriers.

3.4 Debris Mobility Analysis

At present, a computer program for simulation of the entire process of debris filling up the retention zone of a barrier and subsequently overtopping the barrier is not available. It is suggested that simulation of debris dynamics for the design of multiple barriers could be carried out based on a ‘staged mobility analysis’ comprising the following key steps:

- (i) carry out debris mobility analysis using a suitable program (e.g. 2d-DMM or DAN-W) to simulate the dynamics of landslide that travels from the source to the first barrier;
- (ii) use the results of the mobility analysis to determine the velocity at which the debris will launch into a ballistic flight from the crest of the barrier;
- (iii) calculate the geometry of the ballistic trajectory path and the debris velocity after landing;
- (iv) carry out debris mobility analysis to model the landslide debris travelling from the landing position to the next barrier;
and
- (v) repeat Steps (ii) to (iv) until landslide debris reaches the terminal barrier.

When a landslide impacts on a barrier, a portion of the debris is trapped and retained behind the barrier, which absorbs kinetic energy. Once the barrier retention zone is fully filled, the remaining debris launches into a ballistic flight from the crest of the barrier,

carrying the kinetic energy of the remaining landslide debris. For a robust estimate of the length of debris trajectory (x_i , see also Figure 3.3), the velocity at which the debris launches into a ballistic flight (see also Step (ii) above) may be taken as the maximum velocity of the remaining debris (v_m), which is in horizontal direction.

In the most common situation, the above assumption would be conservative and produce a more critical x_i , since the surface of the debris deposit behind an intermediate barrier is likely to be sloping at a lower angle than the natural channel. However, there may be rare cases where the angle of debris deposition behind a barrier would exceed the inclination of the natural channel due to reasons such as excavation into the channel to form a steeper profile for the purposes of increasing the retention volume. However, with a fairly high value of R as recommended (see Equation 3.3), the assumption of horizontal v_m should still produce conservative results in most cases.

The v_m value can be obtained from the velocity output of the debris mobility analysis. For example, if the Lagrangian type mobility model (e.g. 2d-DMM) is used, the mass blocks that would be trapped by the barrier would be those at the front of the debris chain with a volume equal to the retention capacity of the barrier, and the maximum velocity of the remaining mass blocks would be used for trajectory length calculation. The v_m is taken as maximum velocity parallel to channel slope and assumed to act in horizontal direction. In the most common situations, the above assumption would be conservative and produce a more critical x_i , since the surface of the debris deposit behind an intermediate barrier is likely to be sloping at a lower angle than the natural channel.

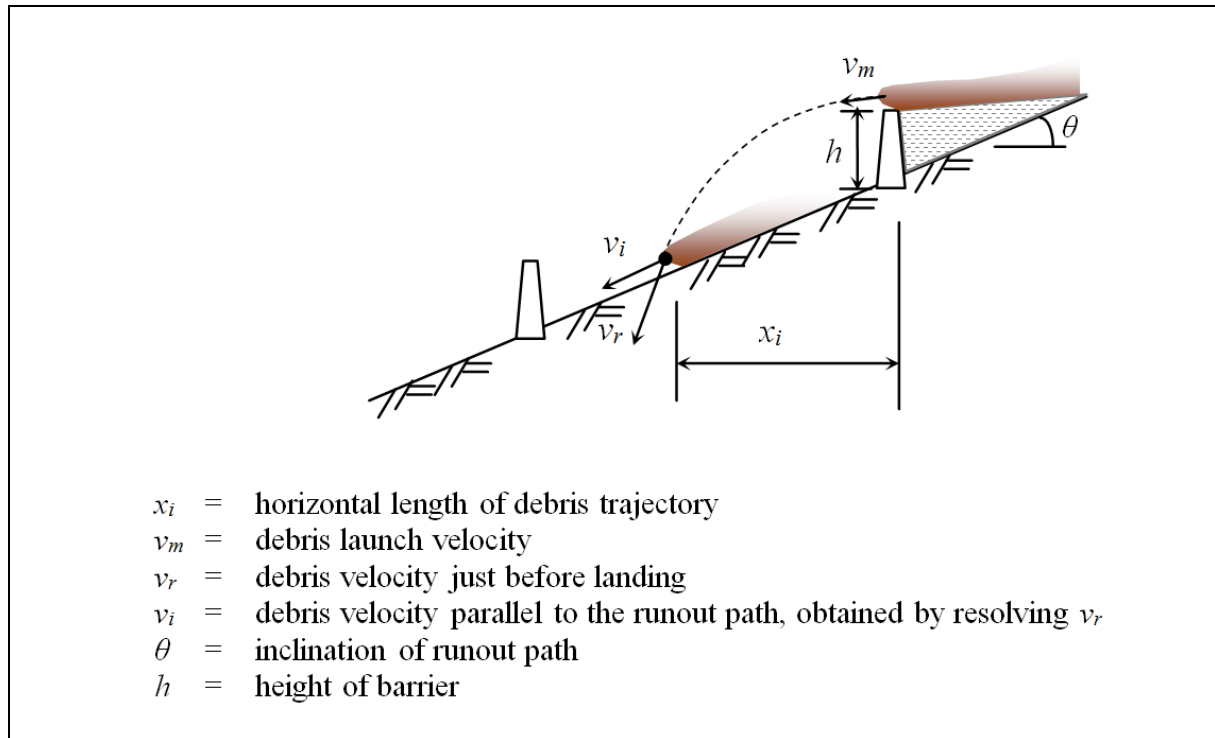


Figure 3.3 Design Parameters for Assessing Dynamic Motion of Landslide Debris Overflowing from a Barrier

With debris launching velocity, v_m (in m/s) in horizontal direction, height of barrier, h (in m), and inclination of the ground profile, θ (in degree), the length of debris trajectory, x_i (in m) can be calculated using Equation 3.1 below, which is derived from energy conservation principle:

$$x_i = \frac{v_m^2}{g} \left[\tan \theta + \sqrt{\tan^2 \theta + \frac{2gh}{v_m^2}} \right] \dots\dots\dots (3.1)$$

The above equation has also been used to calculate the length of debris trajectory of the HKUST's flume tests. It is noted that the equation provides a reasonable estimate as compared with the test results (see Appendix A). For the design of multiple flexible debris-resisting barriers, the reduced height of barrier after debris impact should be used to determine the value of h (see Geobruigg, 2012).

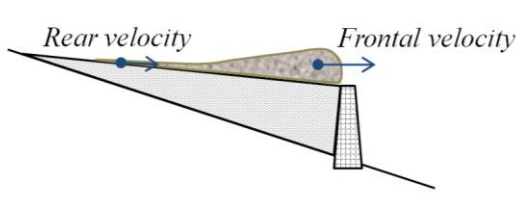
The debris velocity just before landing, v_r (in m/s), is calculated based on the kinetic energy of the remaining debris and the kinetic energy gained in the drop from height as follows:

$$v_r = \sqrt{\frac{2 [C_r KE_r + m_r g (h + C_x x_i \tan \theta)]}{m_r}} \dots\dots\dots (3.2)$$

where m_r = mass of remaining debris (in kg)
 KE_r = kinetic energy of remaining debris (in J)
 C_r = empirical coefficient (≤ 1.0)
 C_x = correction factor on x_i .

The remaining debris mass (m_r) relates to the amount of debris that cannot be trapped by the barrier, i.e. the total volume of debris before hitting the barrier less the barrier retention capacity. The kinetic energy of the remaining debris (KE_r) can be obtained based on the mass and velocity of the remaining mass blocks calculated from the debris mobility analysis. This calculation of kinetic energy of the remaining debris in this way may lead to over-estimation. This is because debris impacting on a barrier can result in rebound of a certain amount of materials and the process could lead to mixing and turbulence of the materials which may involve additional energy dissipation. An empirical coefficient, C_r , is thus proposed to account for this effect. The value of C_r depends on many factors including barrier stiffness, characteristics of the debris, velocity of debris, etc. If no site-specific study of C_r is carried out, it is prudent to assume $C_r = 1.0$ for design purposes. x_i is the maximum projectile distance which defines the landing position of the frontal portion of the remaining debris as it is calculated based on the maximum velocity of the remaining debris. Since the velocity of debris varies, a correction factor C_x is applied to x_i in the equation for the sake of calculating the average projectile length of the overflow. The value of C_x depends on the ratio of the rear velocity to frontal velocity of the remaining debris. Suggested values of C_x , based essentially on a parametric study of projectile lengths over different combinations of barrier height and debris velocity, are listed in Table 3.1 below:

Table 3.1 Suggested Values of C_x

Ratio of Rear Velocity to Frontal Velocity of the Remaining Debris	C_x	
< 0.2	0.6	
0.2 to 0.66	0.8	
≥ 0.67	1.0	

For carrying out the mobility analysis of landslide debris downstream as stated in Step (iv) above, an initial debris velocity is required. This velocity, v_i (in m/s), can be obtained by resolving v_r as shown below:

$$v_i = R v_r \cos \left[\left[\tan^{-1} \sqrt{\frac{m_r g (h + C_x x_i \tan \theta)}{KE_r}} \right] - \theta \right] \dots \dots \dots (3.3)$$

where R = correction factor.

In order to consider the velocity reduction due to the debris impacting on the trail at the landing position, a correction factor of R should be applied to the above equation. As discussed in Section 2.3, the ratio of velocity parallel to debris trail after and before landing could range from 0.3 to 0.75. As the flow dynamics of debris impacting on the ground could be very complex, it is not easy to define precisely the value of R based on the current state of knowledge. It is therefore recommended using a value of R of at least 0.7 to produce a more robust design to cover the large uncertainties involved. When more data become available, the value of R may be reviewed.

Debris mobility analysis to model the dynamics of landslide debris travelling from the landing position to the next barrier would be carried out as per Step (iv) above. x_i , as mentioned above, gives the initial position at which the debris mobility analysis would commence, and v_i gives the initial velocity of debris for the subsequent analysis. Another two parameters, i.e. debris length (x_d) and debris thickness (h_m), are required for carrying out the analysis.

The length of debris, x_d , is assumed to be the same as that of the remaining debris before the overflow (i.e. the length of mass blocks that would not be trapped by the barrier). If the length of debris is greater than the length of debris trajectory (i.e. $x_d > x_i$), for calculation purpose the debris is taken to extend backward from the point of landing to beyond the barrier (x_d in Figure 3.4). Though this is an idealization, it is more robust for design as the debris would start motion again with a higher potential energy. An additional reason for adopting x_d as opposed to x_i is that the latter would have led to greater initial debris thickness for the subsequent mobility analysis which could result in unrealistic basal resistance particularly for a Voellmy model.

With the volume of the remaining debris and width of the runout trail, debris thickness, h_m , upon landing can then be calculated or determined using the pre-processing function ‘Landslide Mass Generator’ in 2d-DMM. In order to simulate a greater debris frontal thickness as normally observed, it is suggested that the maximum thickness of the remaining debris at the debris front should be adopted (i.e. thickness of the first three mass blocks at the front is taken to be the maximum thickness of the remaining debris). The debris thickness then tails off, matching the volume of the remaining debris. However, if the maximum thickness of the remaining debris is less than 0.3 m, calculation using numerical debris mobility models like 2d-DMM and DAN-W may not be able to capture the actual debris dynamics. Hence, use of the proposed debris mobility analysis for simulation of debris dynamics is not recommended in such cases.

2d-DMM (version 1.2) has been developed to allow the input of the above-mentioned initial conditions (i.e. v_i , x_i , h_m and x_d) for modelling debris motion from the landing position to the barrier downhill. The impact velocity of landslide debris at the downhill barrier can be calculated by means of debris mobility analysis.

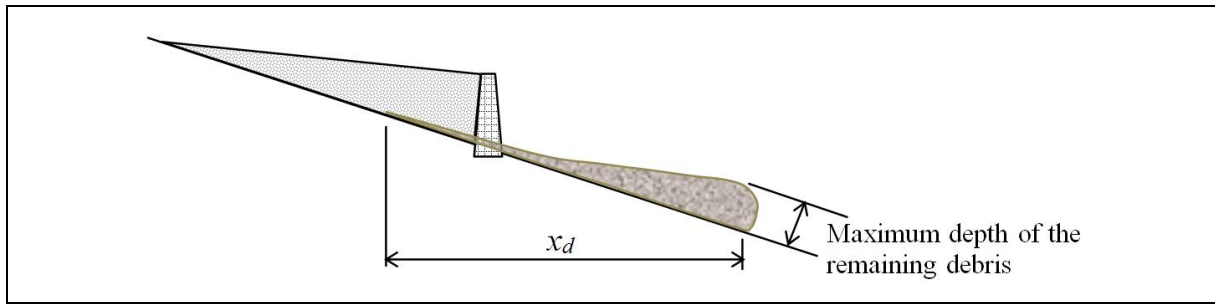


Figure 3.4 A Case where the Length of Debris is Longer than the Length of Debris Trajectory

3.5 Barrier Location

Multiple barriers should be sited at strategic locations such that landslide hazards are mitigated efficiently and effectively. The minimum spacing between two consecutive barriers should be greater than the length of debris trajectory from the upper barrier, x_i . Given the large uncertainty in the assessment of debris trajectory, the minimum spacing between two consecutive barriers should incorporate a certain margin greater than x_i . Otherwise, landslide debris could shoot over the downstream barrier and not be intercepted at all.

According to Zhou et al (1991), VanDine (1996) and SWCB (2005), the minimum spacing between two consecutive barriers should also satisfy the criteria shown in Figure 2.1, in order to avoid any adverse effects of back-waves on the upstream barrier.

It should also be noted that the trajectories of any overflow debris should be confined within the intended runout paths. As a good practice, barriers should not be constructed close to sharp bends of a drainage line so as to guard against possible overshooting of debris to adjacent hillsides. Otherwise, additional precautionary measures such as deflector walls should be provided.

Barriers should not be sited at locations of steep hillside gradient that would limit their retention capacity and at the same time, increase the drop height of overflow debris. Locations of barriers on soft ground should also be avoided to minimise the amount of downstream scouring, which could result in toe instability of barriers.

Multiple barriers may alternatively be located within the deposition zone of a drainage line, where the ground profile is usually gentler (e.g. less than 15°), and where a larger retention capacity can be achieved and a lower debris impact velocity is anticipated.

4 Other Design Considerations

4.1 Intermediate and Terminal Barriers

In order to avoid any adverse effects on the hydraulic capacity of the landslide trail (e.g. natural drainage line), intermediate barriers could be designed as drained structures. Different types of debris-straining structures, such as lattice structures and flexible barriers (see Figure 4.1) may be considered in this regard (Shum & Lam, 2011). Depending on the nature of the debris (e.g. water content and grain size), some frontal portions of the debris could pass through these barriers. The proportions of debris passing through the openings should be duly considered in the design. When rigid barrier is used, adequate drainage for discharge of runoff and water within the retained debris should be provided.



Figure 4.1 Lattice Structure and Flexible Barrier

A terminal barrier refers to the last barrier and serves as an ultimate stop to trap and retain all the debris overflowing from the uphill barriers and to prevent uncontrolled discharge of debris and water to downstream. To fulfill these functions, a terminal barrier should have a retention capacity that is large enough to contain the probable volume of debris overflow from the preceding intermediate barriers, and a non-drained structure is preferred.

4.2 Drainage Provisions

Landslide debris, especially those in channelized debris flows, usually contains a substantial amount of water. For closed type barriers, adequate drainage provisions should

be provided to drain the water from landslide debris as fast as possible once it is entrapped by a barrier. This would encourage the consolidation of landslide debris and thus reduce its bulk volume (i.e. the volume of water and debris). This is important in retaining the pre-defined volume of debris only within the barrier retention zone in minimising the amount of overflowing debris to the terminal barrier.

Flexible barriers consist of ring nets or diagonal wire nets, which are considered as free-draining. Adequate drainage provisions immediately downstream of a terminal flexible barrier should be provided to properly discharge water from debris to suitable outlets nearby.

Surface drainage or ditch in front of terminal barrier should be provided to collect runoff and any fines that may pass through the barrier. This helps to minimise the possibility of the downstream facilities being affected. Special attention should be paid to the use of flexible barrier as a terminal barrier, and the possible volume of debris passing through the barrier should be duly considered. The surface drainage provision should have sufficiently large drainage capacity to convey runoff to designated discharge points, taking into account the possible blockage due to debris or fines being washed down to the drainage.

4.3 Downstream Scouring

Downstream scouring may occur in front of barriers due to overflow of debris. It is good practice to site barriers on relatively firm ground so as to minimise the amount of downstream scouring. Notwithstanding this, downstream scouring may be inevitable in some cases as landslide debris drops from height and dissipates its large amount of energy upon landing before moving downhill. The possibility and extent of downstream scouring should therefore be taken into account in the stability check of barriers. The potential and extent of downstream scouring should also be controlled through the provision of erosion protection measures in the expected scouring zone, which may take the form of gabion mat or other appropriate means as described by Franks & Woods (1997). It is also noted that in overseas practice, an auxiliary dam may be provided immediately downstream of a barrier in order to prevent scouring (CGS, 2004). In all cases, aesthetics should be duly considered in the choice of erosion protection measures.

Chatwin et al (1994) pointed out that lateral stream erosion and scouring by water from spillway could be main causes of check dam failures. Suitable barrier detailing, such as provision of an overflow weir, should be considered for multiple barriers straddling across drainage lines to guard against side scouring. Such details should be designed to cater for the peak discharge of both surface water flow and debris flow (Mizuyama & Ishikawa, 1988; VanDine, 1996).

The geometry of the runout path should be examined in a three-dimensional sense when determining the locations that require scouring protection. For example, when the alignment of the concerned drainage line is not straight, debris overflowing from barrier may hit the bank of the drainage line before landing. Appropriate protection to the bank should therefore be provided.

4.4 Detailing

The following items should be duly considered in the planning and design of multiple barriers:

- (a) drag forces induced by debris overflow should be considered in the design of intermediate barriers; relevant guidelines on drag force calculation are given by Kwan (2012) and Kwan & Cheung (2012);
- (b) barriers with an inclined back should be avoided as it may result in ski-jump of debris;
- (c) a deflector should be provided at the terminal barrier top to prevent debris splash potentially spilling over the barriers (see Kwan, 2012);
- (d) in order to provide confinement to the debris, the crest level of intermediate barriers should not be flush with or should not be higher than the edge of the drainage line (see Figure 4.2);
- (e) erosion control measures (e.g. gabion erosion control mats) on banks of drainage line at upstream of barriers, which may be affected by debris overflow, should be provided; and
- (f) secondary mesh should be provided to minimise fines passing through the nets of the flexible barriers.

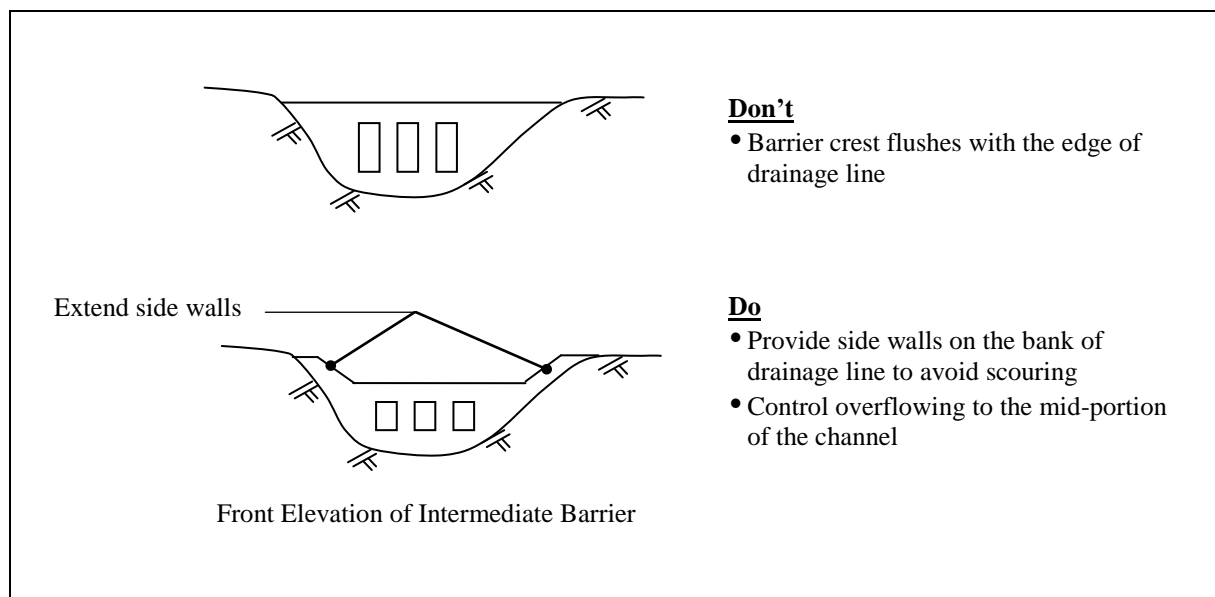


Figure 4.2 Detailing of Barriers

5 Illustrative Examples

Worked examples illustrating in a step by step manner and the suggested work flow of the proposed framework for design of multiple barriers are given in Appendix B.

Key observations from the worked examples are summarized below:

- (a) The use of multiple barriers may not necessarily result in a significant reduction in impact velocity on barriers. This is because of the gains in potential energy when debris overflows from the barrier crest. However, multiple barriers would reduce the design debris impact thickness and hence debris impact load of barriers downstream.
- (b) If Voellmy rheology is assumed, debris velocity determined using the suggested staged approach is found to be not very sensitive to the value of R (see Example 1), as Voellmy fluid would approach a terminal velocity for a given topography setting irrespective of the initial debris velocity.
- (c) In order to prevent debris overflowing the barrier crest from gaining substantial potential energy, the height of intermediate barriers should not be excessive. In the present suggested design procedures, velocity reduction to debris overflowing from a barrier is applied to take into account the effect of debris impact upon landing. However, in general, this velocity reduction may not offset the effect of gain in potential energy for barriers higher than 3 m to 4 m, particularly when the debris runout trail is steep.
- (d) The use of intermediate barriers of a limited height has the advantages of a shorter projectile length and smaller debris impact velocity at the landing position, which could result in lesser scouring of the downstream area.

6 Discussion

Debris overflowing from a barrier launches into a ballistic flight. The overflowing materials gain potential energy and at the same time are not subject to basal resistance during the flight. The gain would increase when the debris runout path is steep, since a steeper runout profile would result in a larger drop height. In order to minimise the gain in potential energy, barrier height should not be too large.

The potential in using multiple barriers to reduce structural requirements and material and construction costs may not be particularly appealing. The site setting also plays an important role in this respect. Since typical drainage lines are generally more incised and steeper in the upper part of catchments than in the lower part, intermediate barriers installed in the upper part of catchment, in particular the first intermediate barrier, would likely be

impacted by debris travelling at a high velocity. As a result, the structural requirements and material and construction costs would be higher.

Multiple barriers can best be located within its deposition zone where the slope gradient is gentler and debris velocity lower. In that case, there is a higher possibility for landslide debris to attain a manageable debris velocity and kinetic energy, in particular for barriers downstream of the first intermediate barrier. Designers may therefore choose to adopt less structurally-demanding barriers, in particular at remote areas where mobilization of plant and construction materials for building a rigid barrier is difficult.

Closely-spaced small-size multiple barriers are mostly not a practicable option to mitigate landslide hazards in Hong Kong. Since the landslide debris usually moves downhill at a velocity close to or above 10 m/s, landslide debris would easily shoot over the closely-spaced multiple barriers and not be intercepted at all.

Overseas experience suggests that multiple barriers can potentially be a practicable option to mitigate reasonably large scale landslides. This may be of relevance to the mitigation of low-frequency, large-magnitude landslides (i.e. in sizable catchments with major drainage lines). Based on the present study, it is observed that the use of multiple barriers in the setting of the natural terrain in Hong Kong could also possibly be a feasible and appealing option to address a number of non-technical concerns that cannot be resolved easily by the use of a single barrier. For example, the use of several barriers smaller in height than a single barrier could provide an effective means to alleviate the possible visual impact of a high single barrier.

The proposed design framework for multiple barriers serves as a starting point to examine the potential use of multiple barriers to mitigate natural terrain landslides in Hong Kong. The proposed design framework should not be regarded as a mandatory standard for multiple barrier design. It is proposed as an option and reference for designers to consider. Designers may choose to adopt other appropriate design methodology, which has been suitably calibrated or verified, for their multiple barrier designs. The design method as suggested by Professor O. Hungr of the University of British Columbia involving the use of software package DAN-W can also be considered.

It should be noted that a simplified design approach involving mobility analysis which does not consider the presence of multiple barriers may be acceptable, provided that there is no increase in the kinetic energy of debris overflow due to the drop at any intermediate barriers. Designer may use Equation 3.3 to calculate the debris velocity at landing to establish the kinetic energy of debris after overflow. The kinetic energy can then be compared with the KE_r (i.e. the kinetic energy before overflow). In addition, the design should follow the minimum spacing requirement as illustrated in Figure 2.1.

A number of design assumptions made in the present proposed design framework, in particular those involved in the calculation of debris trajectory and impact velocity of debris, may need further review and refinement in the light of improved knowledge and additional information or test data. In the suggested design framework, energy dissipation resulting from debris impact on barriers has not been considered. In theory, debris impact on barriers would result in the rebound of a certain amount of material upstream. The process could involve a mixing of materials which may lead to an additional energy dissipation. In

addition, there is a lack of comprehensive research on the energy loss of debris overflowing from a barrier and impacting on the ground.

6.1 Suggestions on Further Work

Further work in the design of multiple barriers and pertinent points warranting attention are summarised below:

- (a) research work on the energy loss of debris impacting on barrier and the ground, and turbulence effect, by means of such as flume tests or field monitoring should be carried out;
- (b) the observed velocity reduction in the flume test experiment could be verified by advance numerical modelling;
- (c) advance numerical tools should be calibrated, e.g. by relevant experimental or field tests, for use as a design tool;
- (d) further studies may be required to investigate the percentage of fines that can be escaped from the flexible barrier and its implication to the design;
- (e) the effect of possible scouring due to debris overflow on the subsequent flow characteristic and the best means to prevent scouring deserves further investigation; and
- (f) data on the angle of debris deposition behind barriers in Hong Kong should be collated with a view to establishing design values for local conditions and practice.

7 Conclusions

The use of multiple barriers on the hillsides in Hong Kong could be a feasible option for certain design scenarios. A preliminary framework for design of multiple barriers has been developed, and illustrated with the use of two worked examples. Areas deserving further work have been put forward.

8 References

- CGS (2004). *Design Code for Debris Flow Disaster Mitigation Measures (DZ/T0239-2004) (Draft)*. China Geological Survey, 59 p. (in Chinese)
- Chatwin, S.C., Howes, D.E., Schwab, J.W. & Swanston, D.N. (1994). *A Guide for Management of Landslide-prone Terrain in the Pacific Northwest (Second Edition)*. Land Management Handbook No. 18, Ministry of Forest, Victoria, British Columbia, Canada, 220 p.

- Chen, X., Li, D. & Cui, P. (2009). Calculation buried depth of transverse sills for the debris flow drainage groove with soft foundation. *Journal of Hefei University of Technology*, vol. 32, no. 10, pp 1590-1605. (in Chinese)
- Cui, P. (2012). Personal communication.
- Franks, C.A.M. & Woods, N.W. (1997). *Natural Terrain Landslide Study Preliminary Review of Natural Terrain Landslide Hazard Mitigation Measures (GEO Technical Note No. 8/97)*. Geotechnical Engineering Office, Hong Kong, 52 p.
- GEO (2013). *Guidelines on Enhanced Approach for Natural Terrain Hazard Studies (GEO TGN 36)*. Geotechnical Engineering Office, Hong Kong, 18 p.
- Geobruigg (2012). *Flexible Shallow Landslide Barriers: Cost-effective Protection against Natural Hazards*. Geobruigg, 12 p.
- Hungr, O. (1995). A model for the runout analysis of rapid flow slides, debris flows and avalanches. *Canadian Geotechnical Journal*, vol. 32, pp 610-623.
- Kwan, J.S.H. (2012). *Supplementary Technical Guidance on Design of Rigid Debris-resisting Barriers (Technical Note No. TN 2/2012)*. Geotechnical Engineering Office, Hong Kong, 85 p.
- Kwan, J.S.H. & Cheung, R.W.M. (2012). *Suggestions on Design Approaches for Flexible Debris-resisting Barriers (Discussion Note No. DN 1/2012)*. Geotechnical Engineering Office, Hong Kong, 90 p.
- Kwan, J.S.H. & Sun, H.W. (2006). An improved landslide mobility model. *Canadian Geotechnical Journal*, vol. 43, pp 531-539.
- Lin, P.S., Lin, J.Y., Chan, K.F. & Chou, W.H. (2007). An experimental study of the impact force of debris flows on slit dams. *Proceedings of the Fourth International Conference on Debris-Flow Hazards Mitigation: Mechanics, Prediction, and Assessment*, Chengdu, China, pp 647-657.
- Mancarella, D. & Hungr, O. (2010). Analysis of run-up of granular avalanches against steep, adverse slopes and protective barriers. *Canadian Geotechnical Journal*, vol. 47, pp 827-841.
- Mizuyama, T. & Ishikawa, Y. (1988). *Technical Standard for the Measures against Debris Flow (Draft)*. Technical Memorandum of PWRI No. 2632, SABO (Erosion Control) Division, SABO Department, Public Works Research Institute, Ministry of Construction, Japan, 57 p.
- Nakatani, K., Wada, T., Satofuka, Y. & Mizuyama, T. (2008). Development of “Kanakano 2D (Ver.2.00)”, a user-friendly one- and two-dimensional debris flow simulator equipped with a graphical user interface. *International Journal of Erosion Control Engineering*, vol. 1, no. 2, pp 62-69.

- NILIM (2007). *Manual of Technical Standard for Establishing Sabo Master Plan for Debris Flow and Driftwood*. Technical Note of NILIM No. 364, Natural Institute for Land and Infrastructure Management, Ministry of Land, Infrastructure and Transport, Japan, 18 p. (in Japanese)
- Osti, R., Itoh, T. & Egashira, S. (2007). Control of sediment run-off volume through close type check dams. *Proceedings of the Fourth International Conference on Debris-flow Hazards Mitigation: Mechanics, Prediction, and Assessment*, Chengdu, China, pp 659-667.
- Shum, L.K.W. & Lam, A.Y.T. (2011). *Review of Natural Terrain Landslide Risk Management Mitigation Measures (Technical Note No. TN 3/2011)*. Geotechnical Engineering Office, Hong Kong, 167 p.
- Speerli, J., Hersperger, R., Wendeler, C. & Roth, A. (2010). Physical modeling of debris flows over flexible ring net barriers. *Proceedings of the Seventh International Conference on Physical Modelling in Geotechnics (ICPMG)*, Zurich, Switzerland, 6 p.
- SWCB (2005). *Soil and Water Conservation Handbook (水土保持手冊)*. Soil and Water Conservation Bureau of the Council of Agriculture, Executive Yuan and Chinese Soil and Water Conservation Society, 692 p. (in Chinese)
- VanDine, D.F. (1996). *Debris Flow Control Structures for Forest Engineering*. Ministry of Forest, Victoria, British Columbia, Canada, 68 p.
- Volkwein, A., Wendeler, C. & Guasti, G. (2011). Design of flexible debris flow barriers. *Proceedings of the Fifth International Conference on Debris-Flow Hazards Mitigations: Mechanics, Prediction and Assessment*, Padua, Italy, pp 1093-1100.
- Wendeler, C. (2008). *Murgangrueckhalt in Wildbächen - Grundlagen zu Planung und Berechnung von Flexiblen Barrieren. Debris Flow Design and Calculation of Flexible Barriers*. PhD thesis, TU Munchen (TU), Switzerland, 288 p. (in German)
- Wendeler, C. (2010). *DEBFLOW - The Dimensioning Tool for Flexible Ring Net Barriers against Debris Flows*. Geobrug, 28 p.
- Wendeler, C., Haller, B. & Salzmann, H. (2012). Protection against debris flows with 13 flexible barriers in the Milibach River (Canton Berne, Switzerland) and first event analysis. *Proceedings of AGS Seminar on Natural Terrain Hazards Mitigation Measures 2012*, Hong Kong.
- White, D.J., Take, W.A. & Bolton, M.D. (2003). Soil deformation measurement using particle image velocimetry (PIV) and photogrammetry. *Geotechnique*, vol. 53, pp 619-631.
- Wong, H.N. (2009). Rising to the challenges of natural terrain landslides. *Proceedings of the HKIE Geotechnical Division Annual Seminar 2009*, pp 15-53.

- Yang, Q., Cai, F., Ugai, K., Su, Z., Huang, R. & Xu, Q. (2012). A simple lumped mass model to describe velocity of granular flows in a large flume. *Journal of Mountain Science*, vol. 9, pp 221-231.
- Yang, Q., Cai, F., Ugai, K., Yamada, M., Su, Z., Ahmed, A., Huang, R. & Xu, Q. (2011). Some factors affecting mass front velocity of rapid dry granular flows in a large flume. *Engineering Geology*, vol. 122, pp 249-260.
- Zhou, B.F., Li, D.J., Luo, D.F., Lu, R.R. & Yang, Q.X. (1991). *Debris Flow Prevention Guide (Chapter 9)*. Chengdu Earth Risk and Environment Research Institute, pp 133-152.

Appendix A

Flume Tests by the Hong Kong University of Science and Technology

Contents

	Page No.
Contents	34
List of Tables	35
List of Figures	36
A.1 Introduction	37
A.2 Set-up of the Flume Test	37
A.3 Experimental Results	38
A.3.1 Velocity Reduction at Landing	39
A.3.2 Projectile Length	39
A.4 Reference	40

List of Tables

Table No.		Page No.
A1	Velocity Data for Calculating Velocity Reduction at Landing	39

List of Figures

Figure No.		Page No.
A1	The Flume Set-up	37
A2	High-speed Camera Images	38

A.1 Introduction

The GEO commissioned the Department of Civil and Environmental Engineering of the Hong Kong University of Science and Technology (HKUST) to carry out a series of flume tests to study the dynamics of debris flow obstructed by baffles. As part of the test programme, HKUST was requested to undertake a flume test of debris overflowing from a vertical rigid barrier. This serves as a reference test for comparing the impedance efficiency provided by baffles and rigid barriers.

A.2 Set-up of the Flume Test

A 5 m long flume with a channel base width of 0.2 m was used (see Figure A1). Side walls are about 0.5 m in height, perpendicular to the channel bed. The channel inclination can be adjusted from 0° (i.e. horizontal) to 55° .

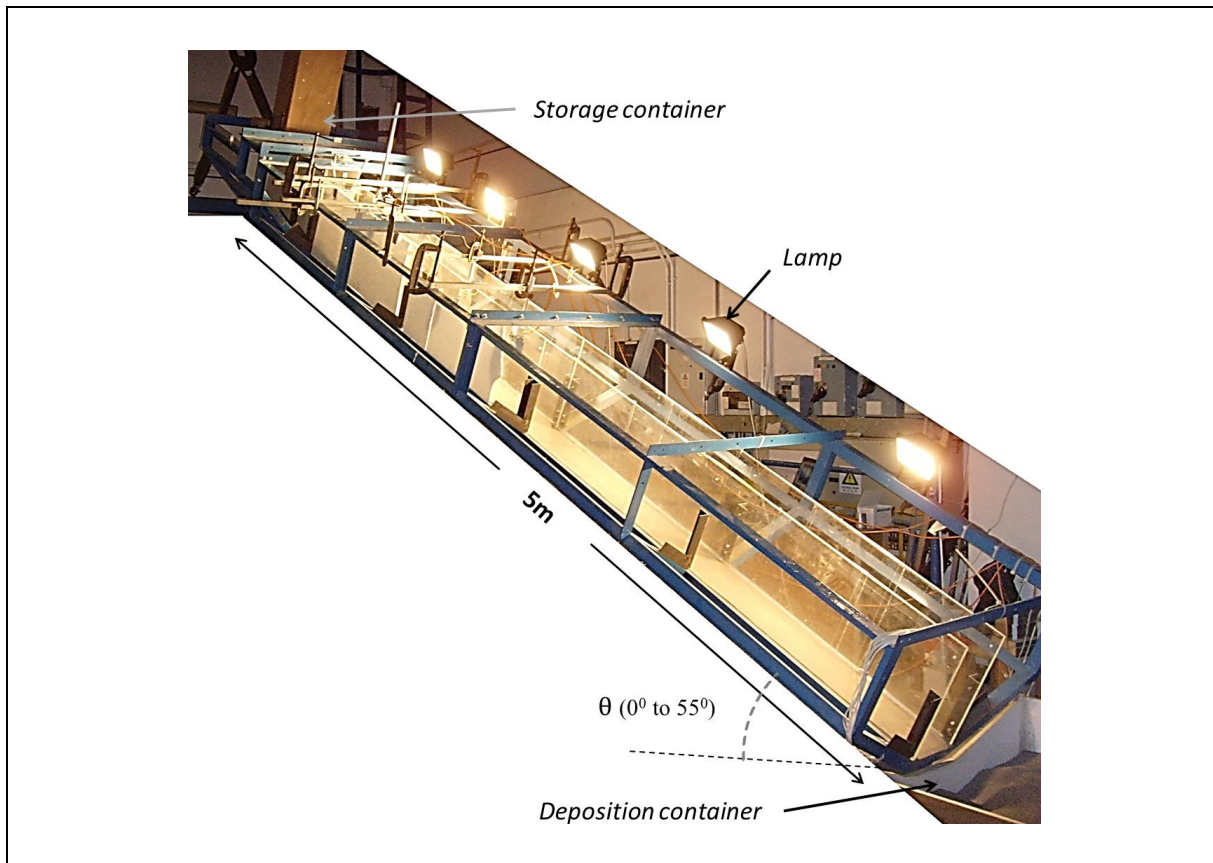


Figure A1 The Flume Set-up

Dry sand was used in the test to form the debris flow. The angle of repose of the sand is 33° and the friction angle between the sand and flume bed is 23° . The initial bulk density of the sand mass is about $1,680 \text{ kg/m}^3$. At the top end of the flume is a sand storage tank. Sand can be released into the flume by opening a flip gate that is attached to the tank.

The vertical barrier model used in the flume test is 0.1 m high and made up of a 10 mm thick aluminum plate. It is firmly secured within the flume at midway of the channel.

Several trials were carried out to establish an appropriate flume inclination. It was subsequently decided that the flume should be inclined at 26° based on the consideration of the Froude number of the sand flow. Froude number ($F_r = v/(g h)^{0.5}$, where v is debris velocity, g is gravitational acceleration and h is debris depth) is a dimensionless parameter usually adopted to characterise the inertia of debris flow. In local design practice, the value of F_r of debris flows in typical design scenarios for barrier design is about 3, given that design impact velocity is about 10 m/s and a flow depth of about 1 m (i.e. $F_r = 10/(10 \times 1)^{0.5} = 3.2$). When the inclination of the flume is 26° , the sand flow in the flume would attain a velocity of about 2.6 m/s with an approaching depth of around 0.08 m at the location of the model barrier. This corresponds to a Froude number of 2.9 ($= 2.6/(10 \times 0.08)^{0.5}$).

A.3 Experimental Results

The flume test was recorded with the use of a high-speed camera which could capture 100 images per second. Figure A2 shows the image records in sequence.

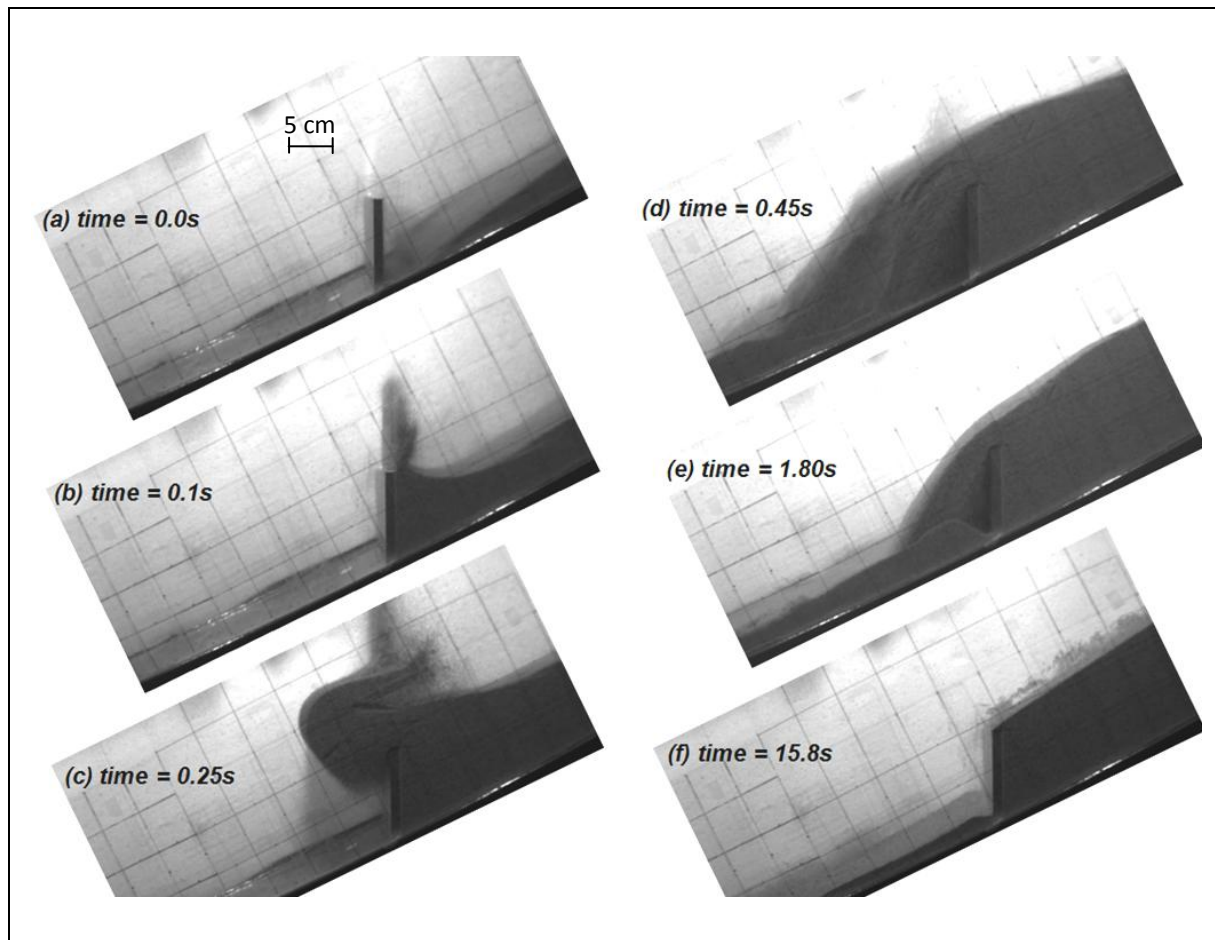


Figure A2 High-speed Camera Images

Figure A2(a) shows the instant when the dry sand flow arrived at the barrier location. For discussion purposes, the time of this instant is denoted as $t = 0.0$ s. After 0.1 second, the sand flow filled up the retention zone behind the barrier and splashing of the sand is also evident. At $t = 0.25$ s, debris that was not trapped behind the barrier started the overtopping process and launched into a ballistic flight. Subsequently, debris overflowing from the crest of the barrier travelled along a projectile path and landed on the flume bed at a distance about 0.2 m downstream of the barrier (see Figure A2(d)). This process continued for about 16 seconds. At the end of the test, sands piled up behind the barrier and the deposition angle was about 33° .

The velocity of the sand flow has been determined using the ‘geoPIV’ computer package developed by White et al (2003). This package is developed based on close-range photogrammetry techniques capable of tracing movements of soil grains captured in high-resolution images. It produces displacement and velocity vectors of the soil grains. Typical results of the PIV analysis are shown in Figure 2.2.

A.3.1 Velocity Reduction at Landing

Velocity reduction upon immediate landing at the end of the ballistic flight has been studied. Table A1 summarises the velocity parallel to the flume before and after landing as well as the velocity ratio. The velocity ratio ranges from about 0.3 to 0.5.

Table A1 Velocity Data for Calculating Velocity Reduction at Landing

Time (s)	Velocity Parallel to the Flume Just <u>Before</u> Landing (V_b) (m/s)	Velocity Parallel to the Flume Immediately <u>After</u> Landing (V_a) (m/s)	V_a/V_b
0.46	1.3	0.6	0.46
0.51	1.4	0.6	0.43
0.61	1.6	0.7	0.44
1.11	1.6	0.4	0.25
1.31	1.3	0.4	0.31

A.3.2 Projectile Length

Equation 3.1 is developed to calculate the length of projectile for debris overflowing from the crest of barrier. The velocity and trajectory length data presented in Figure 2.2 are used to verify this equation. As shown in the figure, debris overflowing velocity at the barrier crest is about 1.0 m/s. Using Equation 3.1, the estimated length of trajectory is 0.18 m. The trajectory length as observed in the test was 0.2 m. This demonstrates that Equation 3.1 is capable of producing a reasonable estimate of the trajectory length.

A.4 Reference

White, D.J., Take, W.A. & Bolton, M.D. (2003). Soil deformation measurement using particle image velocimetry (PIV) and photogrammetry. *Geotechnique*, vol. 53, pp 619-631.

Appendix B

Illustrative Examples

Contents

	Page No.
Contents	42
List of Tables	43
List of Figures	44
B.1 Introduction	45
B.2 Example No. 1	45
B.2.1 Discussion on Example No. 1	49
B.3 Example No. 2	49
B.3.1 Discussion on Example No. 2	58
B.4 Reference	58

List of Table

Table No.		Page No.
B1	Comparison of Numerical Results for Single Barrier and Multiple Barriers	58

List of Figures

Figure No.		Page No.
B1	The Design Event and Runout Profile (Example No. 1)	45
B2	Output of 2d-DMM (Example No. 1)	46
B3	Input of Parameters which Govern the Initial Conditions of Debris Motion (Example No. 1)	48
B4	The Design Event and Runout Profile (Example No. 2)	49
B5	Cross-sectional Profiles at $x = 350$ m and $x = 460$ m	50
B6	Topographic Plan and Aerial Photograph of the Catchment	51
B7	Output of 2d-DMM (Example No. 2)	52
B8	Input of Parameters which Govern the Initial Conditions of Debris Motion (Example No. 2)	54
B9	Output of 2d-DMM for the Second Intermediate Barrier (Example No. 2)	55
B10	Input of Parameters which Govern the Initial Conditions of Debris Motion for the Second Intermediate Barrier (Example No. 2)	57

B.1 Introduction

Two examples are presented in this Appendix to illustrate the procedures put forward in Section 3.4 of the report for the design of multiple barriers. The design event and geometry of the runout profiles considered in Example No. 1 are extracted from a LPMit project. The second worked example pertains to the mitigation measures for the Yu Tung Road catchment, with the design event assumed to be the same as the debris flow that occurred on 7 June 2008.

B.2 Example No. 1

This example considers a channelised debris flow. A section of the runout profile is presented in Figure B1. The inclination of the runout profile ranges from 25° to 45° . The landslide source volume is 450 m^3 . The width of channel is taken to be a constant of 13 m. A barrier of 5.5 m is proposed at chainage $x = 200 \text{ m}$ where the gradient is 26° in the original conforming design.

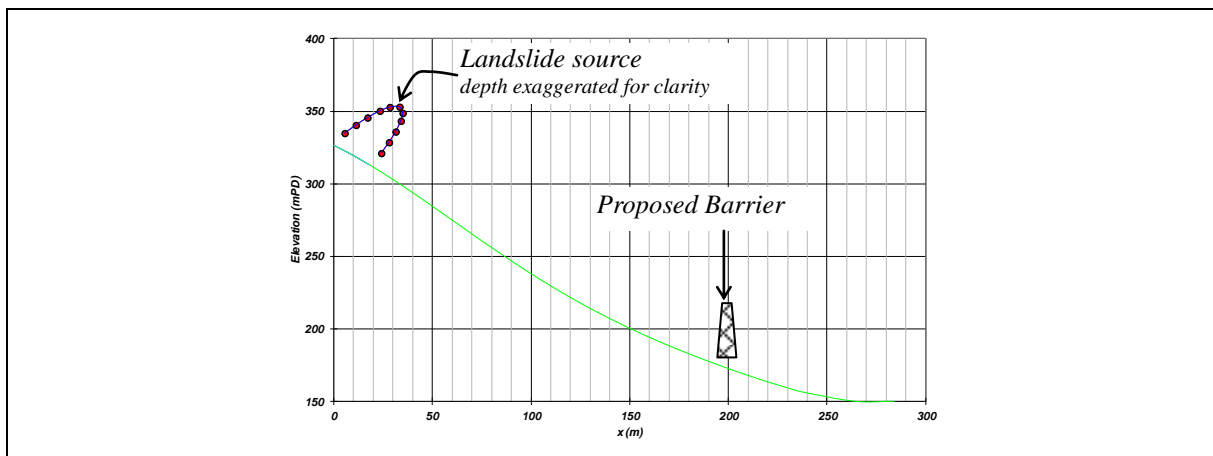


Figure B1 The Design Event and Runout Profile (Example No. 1)

Following the procedures suggested by Kwan (2012), the design impact velocity and design impact thickness is estimated to be 8.0 m/s and 0.4 m respectively. The corresponding design maximum impact load is 126 kN/m based on the combination of debris velocity and thickness. The design landslide density is $1,970 \text{ kg/m}^3$. A dynamic coefficient of 2.5 is assumed for rigid barrier.

To illustrative the suggested design procedure given in Section 3.4, it is assumed that reduction of the barrier height to 3.5 m is required to cope with site constraint. In order to provide adequate debris retention volume, an additional barrier of 2.5 m high at chainage $x = 170 \text{ m}$ is required and the design retention volume of this additional barrier is 140 m^3 . The deposition angle of debris is assumed to be 10° .

The procedure for calculating the design impact velocity and design debris thickness for the barriers at $x = 170 \text{ m}$ and $x = 200 \text{ m}$ is illustrated below.

Step (i) - carry out debris mobility analysis using a program prior accepted by GEO (e.g. 2d-DMM or DAN-W) to simulate the mobility of debris flow travelling from the landslide source to the first barrier.

In this example, the computer program 2d-DMM (Version 1.2) is used to carry out the debris mobility analysis. Debris arrives at the first barrier location at roughly 15.4 seconds after the onset of the landslide. The design debris impact velocity is 9.4 m/s and the maximum debris thickness is 0.45 m. Based on the hydrograph data, the design impact load is calculated to be 195 kN/m.

Sheet 'Results for Post-processing' provides detailed output results, which indicate that at $t = 15.4$ seconds, the frontal debris mass block (i.e. Block 11) reaches $x = 169.5$ m (see part-print of Sheet 'Results for Post-processing' in Figure B2). The five front mass blocks (i.e. Blocks 7 to 11) constitute a volume of 185 m^3 , which is larger than the retention capacity of barrier at $x = 170$ m. Therefore, Blocks 8 to 11 and a portion of Block 7 will be retained by the barrier.

Length of remaining debris = $134 - 52 = 82$

Velocities of remaining debris

Kinetic energy of remaining

A	B	C	D	E	F	G	H	I	J	K	L	M	N	O	P
Time	15.4 sec	UBF	-290.944 kN	Acc	-0.03591903 m/sec ²	Potential	551764.4 kJ	Kinetic	27008.73 kJ	total					
Boundary blocks 1 to 11															
s	x	y	alpha	R	Ent/Dep	B	B	H	Vol	v	k	T	P	F	KE
(m)	(m)	(m)	(radians)	(m)	m ³ per tim (m)	(m)	(m)	(m)	(m ³)	(m/sec)	(kN)	(kN)	(kN)	(kN)	(kJ)
69.21896	52.75294	281.7369	0.760838	-2346.32	0	13.3	13.3	0.033866	6.013194	4.019466	0.842	75.24257	-0.24115	-0.85085	96
84.73682	63.97512	271.0174	0.762556	5241.29	0	13.3	13.3	0.076102	19.33367	4.643525	0.842	243.5138	-0.43253	-3.55355	411
106.9121	80.08725	255.7798	0.749633	1046.081	0	13.3	13.3	0.111823	33.30273	5.54399	0.842	416.533	-0.67852	-8.76464	1008
129.707	96.97963	240.4773	0.7199	611.7713	0	13.3	13.3	0.158109	47.31289	6.500146	0.842	577.8545	-1.26113	-17.6263	1969
151.6199	113.7367	226.3647	0.67806	463.3886	0	13.3	13.3	0.216344	69.4148	7.40308	0.842	815.6383	-2.75285	-34.6216	3747
177.2331	134.1403	210.8988	0.617698	400.9453	0	13.3	13.3	0.318288	89.42182	8.393949	0.842	987.9063	-4.64579	-60.3407	6206
194.7343	148.6203	201.0823	0.573883	403.4709	0	13.3	13.3	0.390867	71.6056	8.999718	0.842	751.7291	-3.92461	-55.9138	5713
204.8863	157.2102	195.6794	0.549209	421.3295	0	13.3	13.3	0.434537	50.15502	9.269715	0.842	511.4546	-2.63189	-42.8183	4245
212.1437	163.4295	191.9452	0.532376	441.8197	0	13.3	13.3	0.459888	35.92391	9.462387	0.842	363.0869	-0.62005	-35.489	3168
216.6518	167.3234	189.6776	0.522352	457.7186	0	13.3	13.3	0.449748	21.03546	9.624435	0.842	221.7484	9.457998	-23.3802	1919
219.1984	169.5329	188.4137	0.51685	467.6864	0	13.3	13.3	0.223996	6.480899	9.733434	0.842	77.94462	12.71439	-7.58529	605

Chainage of mass Block 11

Sum of volume is about 185 m^3

Maximum thickness of remaining debris

Block 1 Debris tail

Block 11 Debris front

Figure B2 Output of 2d-DMM (Example No. 1)

Step (ii) - use the results of the mobility analysis to determine the velocity at which debris will launch into a ballistic flight from the crest of the barrier.

The maximum velocity of the remaining debris would be taken as v_m for calculation of the length of debris trajectory (x_i). According to the calculation of 2d-DMM, the maximum velocity is 8.99 m/s, i.e. 9.0 m/s.

Step (iii) - calculate geometry of the ballistic flight path and the debris velocity after landing.

With $v_m = 9.0$ m/s and channel inclination $\theta = 26^\circ$, with barrier height $h = 2.5$ m, a value of $x_i = 12$ m is obtained by using Equation 3.1. The barrier spacing in this example is 30 m, and this is larger than both the length of projectile (12 m) and the minimum spacing calculated using the formula given in Figure 2.1, which is 8 m.

- (a) Initial debris velocity - this is the debris velocity in the direction of the fall of the drainage line, and it should be input to Cell 'D71' on Sheet 'Input' of 2d-DMM (see also Figure B3). In this example, the initial velocity is 8.3 m/s.
- (b) Initial location of Block 1 - this is the chainage of the rear end of the debris chain and is input to Cell 'H75'. This chainage relates to the location of the barrier (i.e. $x = 170$ m), the length of trajectory (i.e. 12 m) and the total length of the debris chain (in Cell 'D69'). Formula " $= 170 + 12 - D69$ " can be set in Cell 'H75' for automatic calculation of the chainage. The total length of remaining debris before overflowing the barrier, which is 82 m (see Figure B2), is entered to Cell 'D69'.

(c) Volume of debris overflowing from barrier - a value of 310 m^3 ($= 450 \text{ m}^3 - 140 \text{ m}^3$) is entered into Cell 'D70'.

(d) Total length of debris chain - a 'rectangular' debris is assumed, and 'Landslide Mass Generator' can be used to produce a preliminary estimate of debris thickness. User can then modify the thickness of debris in Cells 'D74' to 'D84'. The debris thicknesses of the first two blocks (i.e. Block Nos. 10 and 11) are assigned to be 0.4 m (the maximum thickness of the remaining debris). The thickness tails off towards the debris end to make up the remaining landslide volume of 310 m^3 .

4. Interface Properties			
Flow resistance on side slopes considered? <input type="checkbox"/> (Yes = 1, No = 0)			
Distance x for change from Interface (1) to (2) = 1000 m			
Interface (1)		Interface (2)	
Cohesion	c = 0 kPa	Cohesion	c = 0 kPa
Friction angle	$\phi = 11^\circ$	Friction angle	$\phi = 11^\circ$
Pore pressure ratio	$r_u = 0$	Pore pressure ratio	$r_u = 0$
Turbulence coefficient	$\xi = 500 \text{ m/s}^2$	Turbulence coefficient	$\xi = 500 \text{ m/s}^2$
Entrainment/Deposition (Zone 1)		Entrainment/Deposition (Zone 2)	
Zone 1 starts at x = 1000 m		Zone 2 starts at x = 0 m	
Zone 1 ends at x = 15000 m		Zone 2 ends at x = 0 m	
Entrainment/deposition rate = 0.00 m^3/sec (-ve entrainment)		Entrainment/deposition rate = 0.00 m^3/sec (-ve entrainment; +ve deposition)	
Threshold Depth of Debris for Entrainment = 0 m		Consider Consolidation? <input type="checkbox"/> (Yes = 1, No = 0, if 0 goto Row 68)	
Min. Depth of Debris for Deposition = 0 m		Fraction of Saturated Layer $h_s = 0$ (proportion of debris height, < 1)	
		Coefficient of Consolidation $c_v = 0 \text{ m}^2/\text{s}$	
5. Landslide Mass			
Total Length of the Landslide Mass at Source = 82 m (for Landslide Mass Generator)		6. Analysis Parameters	
Total Volume of the Landslide Mass at Source = 310 m^3 (for Landslide Mass Generator)		Analysis stops at t = 40 s	
Initial debris velocity = 8.3 m/s		Time step interval $\Delta t = 0.02 \text{ s}$	
Input the initial conditions of the landslide mass:			
Boundary block No.	Location, x (m)	Thickness, h (m)	
1	100.0000	0.1000	
2	105.7400	0.1200	
3	112.3000	0.1300	
4	120.5000	0.1600	
5	128.7000	0.1800	
6	141.0000	0.2200	
7	153.3000	0.2700	
8	161.5000	0.3100	
9	169.7000	0.3700	
10	176.2600	0.4000	
11	182.0000	0.4000	
Volume of landslide mass (m^3)		310	
Landslide Mass Generator			
Parabolic or Rectangular (P/R)? <input type="checkbox"/> (for Landslide Mass Generator)		Location, x of Block No. 1 = 100.0 m	
		Magnification factor for displaying the debris thickness = 20	
		No. of time steps between updating display and output = 10	
Start Analysis			

Note: Deposition Zone 1 starts from $x = 1,000 \text{ m}$ (see Row 60) but the total runout distance in the analysis is about 300 m only, therefore, parameters specified for Zone 1 are irrelevant to the analysis.

Figure B3 Input of Parameters which Govern the Initial Conditions of Debris Motion (Example No. 1)

The program 2d-DMM (version 1.2) takes into account the specified initial conditions to carry out debris mobility analysis. The analysis shows that the debris reaches the second barrier at $x = 200 \text{ m}$ at a velocity of 7.3 m/s and the design debris thickness is 0.35 m (c.f. velocity = 8.0 m/s and debris thickness = 0.4 m when a single barrier is used). The corresponding design impact pressure is 92 kN/m ($\approx 2.5 \times 1,970 \times 7.3^2/1,000 \times 0.35$). This is about 27% less than that in the case of the single barrier design.

Since there are only two barriers, Step (v) given in Section 3.4 is not relevant to this example. The second barrier should also be designed with consideration of possible

landslides occurring at location downstream of the first one (see also Section 3.2). The related mobility analysis would be similar to the one carried out under Step (i) but with the landslide source assumed to be downstream of $x = 170$ m. The corresponding analysis is not included in this illustrative example.

B.2.1 Discussion on Example No. 1

The debris velocity overflowing from the first intermediate barrier is relatively high, at 9.4 m/s. It results in a long projectile path. This prompts the designer to consider the debris flow path in a three dimensional sense. For example, the debris transport channel may not be perfectly straight and debris overflowing from the barrier may impact on channel banks downstream of the barrier.

An additional analysis using $R = 1.0$, with the values of C_r and C_x kept unchanged, has been carried out (detailed calculations are not presented here). The re-calculated debris velocity (v_i) after landing is 11.9 m/s. The analysis shows that the debris reaches the second barrier at $x = 200$ m at a velocity of 7.6 m/s (c.f. 7.3 m/s when $R = 0.7$ is used) and the design debris thickness is 0.35 m. In this example, the design debris impact velocity and design debris impact thickness of the terminal barrier are not sensitive to the assumed value of R .

B.3 Example No. 2

This example considers the channelised debris flow at Yu Tung Road. The debris flow that occurred on 7 June 2008 in the Yu Tung Road catchment is assumed to be the design event. A section of the runout profile is presented in Figure B4. The inclination of the runout profile ranges from 10° to 30° . The design landslide source volume is $3,300 \text{ m}^3$ which is the sum of the original landslide volume and the volume of entrainment during the landslide transport process. The width of channel varied from 4 m to 9 m. A 7 m-high barrier is proposed at chainage $x = 525$ m in the original conforming design.

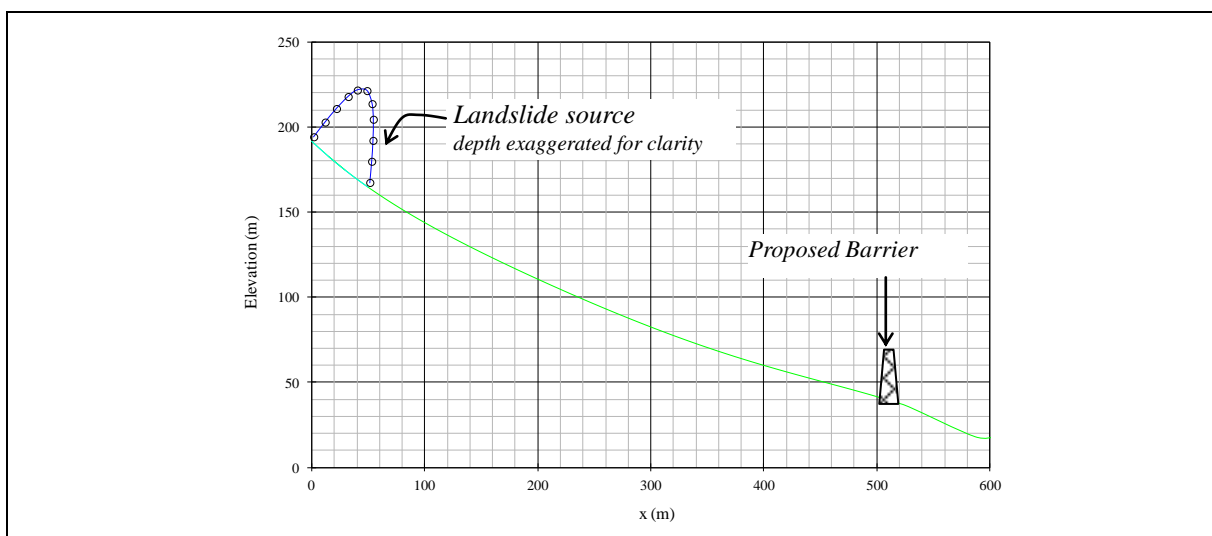


Figure B4 The Design Event and Runout Profile (Example No. 2)

If the procedures suggested by Kwan (2012) are followed, the design impact velocity at the barrier is 7.8 m/s and the design debris thickness is 2.1 m. These design values would combine to give the maximum impact load. The corresponding design impact load is 575 kN/m, assuming a landslide density of $1,800 \text{ kg/m}^3$ and a dynamic coefficient of 2.5.

To illustrate the suggested design procedure given in Section 3.4, it is assumed that reduction of the barrier height from 7 m to 4 m is required. In order to provide adequate debris retention volume, two additional barriers of 3 m high at $x = 350 \text{ m}$ and 460 m respectively are required. The design retention volumes of these two additional barriers are calculated based on the slope gradient (see Figure B4) and the cross-sectional areas at the location of barriers as shown in Figure B5. The deposition angle of debris is assumed to be 10° . The topographical plan and aerial photograph of the catchment together with locations of barriers are shown in Figure B6. The estimated retention volumes for the barriers at $x = 350 \text{ m}$ and $x = 460 \text{ m}$ are 780 m^3 and 710 m^3 respectively.

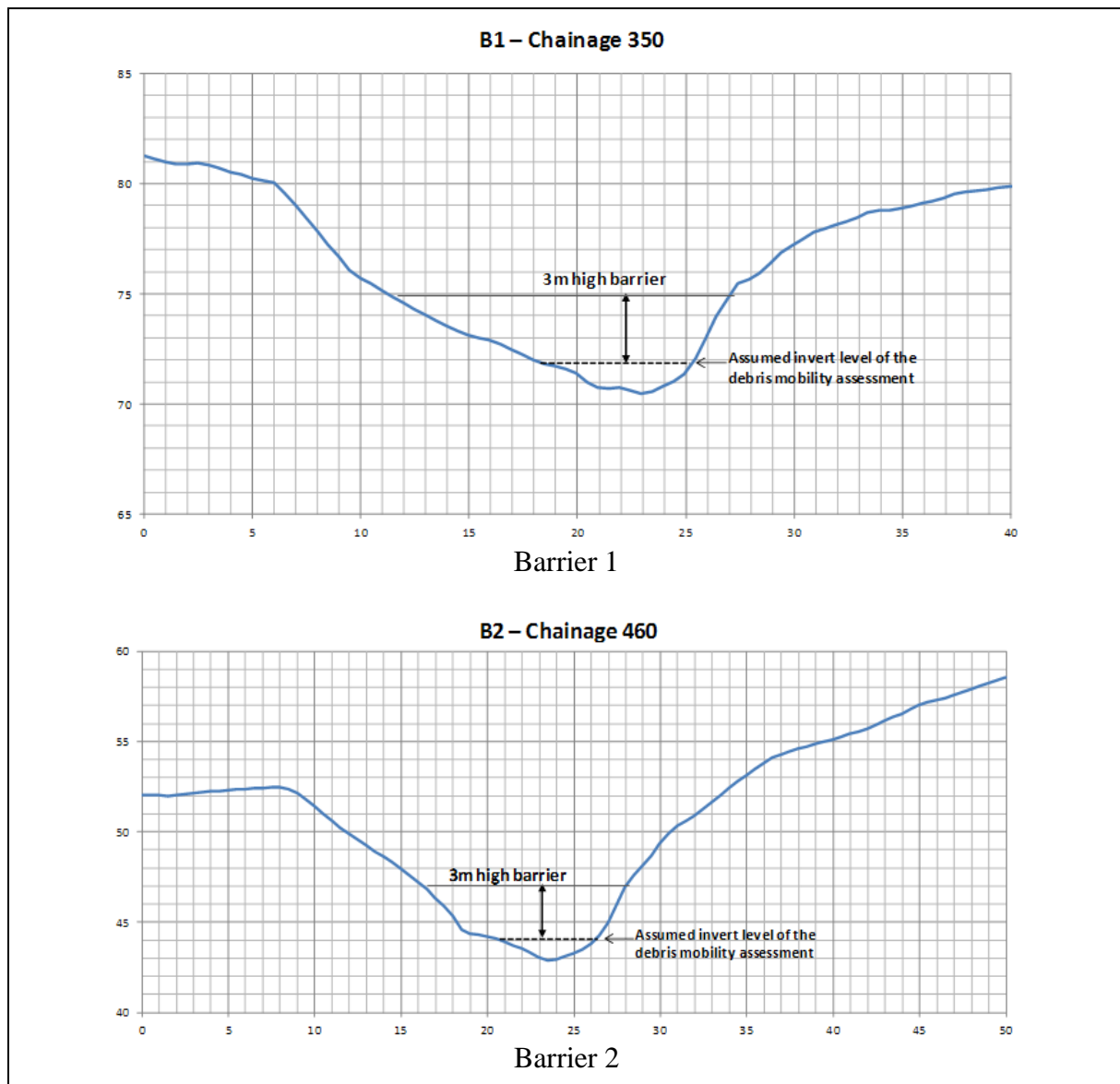
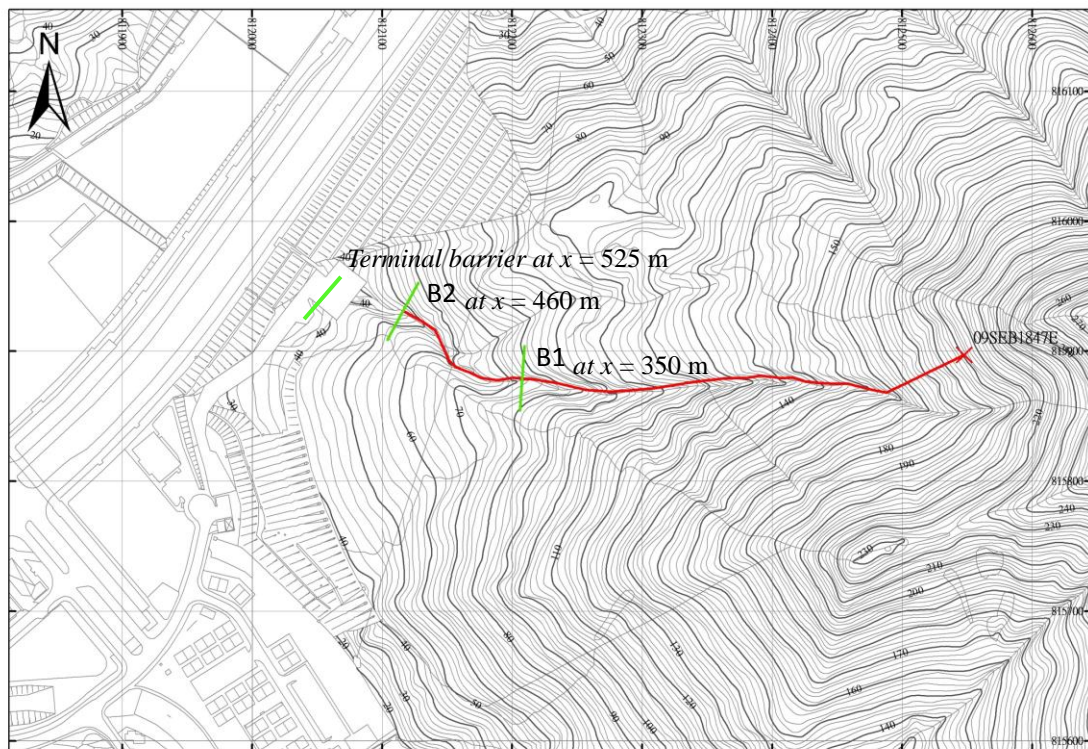


Figure B5 Cross-sectional Profiles at $x = 350 \text{ m}$ and $x = 460 \text{ m}$



Topographic Plan



Aerial Photo

Figure B6 Topographic Plan and Aerial Photograph of the Catchment

The procedures for calculating the design impact velocity and design debris thickness for the first barrier B1 and second barrier B2 are illustrated below.

Step (i) - carry out debris mobility analysis using a program prior accepted by GEO (e.g. 2d-DMM or DAN-W) to simulate the mobility of debris flow travelling from the landslide source to the first barrier.

Debris arrives at the first barrier location ($x = 350$ m) at 22.5 seconds after the onset of the landslide. Based on the hydrograph data (which are not shown herein) and Kwan (2012), the design debris impact velocity is 11.3 m/s and the design debris thickness is 2.8 m. The design impact load is calculated to be 1,610 kN/m.

Sheet 'Results for Post-processing' provides detailed output results for case of debris reaching the first barrier B1, which indicate that at $t = 22.5$ seconds, the frontal debris mass block (i.e. Block 11) reaches $x = 350$ m (see part-print of Sheet 'Results for Post-processing' in Figure B7). The five front mass blocks (i.e. Blocks 7 to 11) constitute a volume of $1,020 \text{ m}^3$, which is larger than the retention capacity of barrier at $x = 350$ m. Therefore, Blocks 8 to 11 and a portion of Block 7 will be retained by the barrier. The remaining volume, which is the entire debris volume of $3,300 \text{ m}^3$ minus 780 m^3 (retention volume of B1), is $2,520 \text{ m}^3$.

Length of remaining debris = $314 - 122 = 192$

Velocities of remaining debris

Kinetic energy of remaining

Time	UBF	-1759.82 kN	Acc	-0.02962668 m/sec ²	Potential	4319.63 kJ	Kinetic	371242.9 kJ	total						
Boundary blocks 1 to 11															
s	x	y	alpha	R	Ent/Dep	B	top width	H	Vol	v	k	T	P	F	KE
(m)	(m)	(m)	(radians)	(m)	m ³ per tim	(m)	(m)	(m)	(m ³)	(m/sec)	(kN)	(kN)	(kN)	(kN)	(kJ)
134.1208	121.7033	135.8021	0.337333	1249.521	0	3.639286	3.813591452	0.198063	21.49907	4.906953	0.959857	131.3399	-1.53475	-4.79416	466
177.8816	163.2058	121.9333	0.30996	2055.576	0	3.648151	4.22200131	0.763259	125.5232	7.065542	0.959857	694.8131	-36.4989	-42.1442	5640
216.1357	199.7324	110.5707	0.293924	2671.215	0	4.267382	5.590922562	1.671517	282.7236	8.789742	0.959857	1445.137	-114.012	-84.8052	19659
247.6928	229.9882	101.6036	0.282354	2703.348	0	4.906854	7.044938628	2.431951	443.8575	10.12409	0.959857	2230.449	-150.939	-155.392	40945
276.8387	258.0244	93.63889	0.271023	2418.566	0	5.843068	9.497377928	2.918513	648.3433	11.04246	0.959857	3263.262	-156.004	-294.961	71151
310.9219	290.9305	84.76006	0.255615	2027.999	0	6.180131	9.6631201	3.179208	507.7885	11.98219	0.959857	2653.573	105.6303	-350.236	65614
335.4117	314.6631	78.71693	0.242823	1818.049	0	6.286316	9.466085455	2.865964	285.1425	12.06506	0.959857	1560.169	166.1001	-203.945	37356
351.0155	329.8254	75.03131	0.234007	1728.502	0	6.338196	8.914971999	2.311004	155.7736	12.2182	0.959857	937.0192	186.7476	-115.664	20929
368.5266	346.8801	71.0583	0.223687	1673.954	0	6.373162	8.182385682	1.617993	61.52376	12.34374	0.959857	444.7315	154.9686	-44.1068	8437
371.3386	349.6228	70.43679	0.222005	1670.167	0	6.384631	7.238583692	0.763026	10.00426	12.38438	0.959857	92.71224	45.92819	-7.13379	1381

Chainage of mass Block 11

Sum of volume is about 1020 m³

Maximum thickness of remaining debris

Block 1 Debris tail

Block 11 Debris front

Figure B7 Output of 2d-DMM (Example No. 2)

Step (ii) - use the results of the mobility analysis to determine the velocity at which debris will launch into a ballistic flight from the crest of the barrier.

The maximum velocity of the remaining debris would be taken as v_m for calculation of the length of debris trajectory (x_i). According to the calculation of 2d-DMM, the maximum velocity is 12.0 m/s.

Step (iii) - calculate geometry of the ballistic flight path and the debris velocity after landing.

With $v_m = 12$ m/s, and channel inclination $\theta = 16^\circ$, and barrier height $h = 3$ m, a value of $x_i = 15$ m is obtained by using Equation 3.1. The barrier spacing between B1 and B2 in this example is 110 m, which is larger than both the length of projectile (15 m) and the minimum spacing calculated using the formula given in Figure 2.1, which is 27 m.

The kinetic energy (KE) of the debris that would not be trapped by the barriers can be calculated as follows (KE of each mass block can be found in Column 'P' of the output sheet, see also Figure B7):

KE of Block 1	=	466 kJ
KE of Block 2	=	5,640 kJ
KE of Block 3	=	19,659 kJ
KE of Block 4	=	40,945 kJ
KE of Block 5	=	71,151 kJ
KE of Block 6	=	94,622 kJ
Sub-total	=	232,482 kJ
KE from Block 7	=	30,999 kJ
Total		= 263,481 kJ

Volume of this block = 508 m³
 Volume of debris that cannot be trapped by barrier = 240 m³
 Total KE of Block 7 = 65,614 kJ
 \therefore KE of the volume escaped
 = 65,614 x 240/508
 = 30,999 kJ

It follows that the KE of the remaining debris (KE_r) i.e. that cannot be retained by the barrier is 263,481 kJ. The remaining debris mass $m_r = (3,300 - 780) \text{ m}^3 \times 1,800 \text{ kg/m}^3 = 4,536,000 \text{ kg}$. Using Equations 3.2 and 3.3, the debris velocities at landing (v_r) and after landing (v_i) are calculated to be 15.9 m/s and 10.4 m/s respectively, by assuming the value of $R = 0.7$, $C_r = 1.0$ and $C_x = 0.8$. (Designers should note that use of a larger value of R may be warranted in design; C_x value is determined from Table 3.1 based on the ratio of the rear velocity (4.9 m/s) to frontal velocity (12.0 m/s) of the remaining debris, see Figure B7.)

Step (iv) - carry out debris mobility analysis to model debris flow travelling from the landing position to the next barrier.

The frontal thickness of debris at landing (h_m) is assumed to be equal to the maximum thickness of the remaining debris (Block 1 to Block 7) before overflowing from the barrier. From the output shown in Figure B7, h_m is 3.4 m and the total length of the landslide mass is assumed to be the length of remaining debris before overflowing from the barrier. The follow parameters are therefore specified for the mobility analysis:

- Initial debris velocity - this is the debris velocity in the direction of the fall of the drainage line, it should be input to Cell 'D71' on Sheet 'Input' of 2d-DMM (see also Figure B8). In this example, the initial velocity is 10.4 m/s.
- Initial location of Block 1 - this is the chainage of the rear end of the debris chain and is input to Cell 'H75'. This chainage relates to the location of the barrier (i.e. $x = 350$ m), the length of trajectory (i.e. 15 m) and the total length of the debris chain (in Cell 'D69'). Formula " $= 350 + 15 - D69$ "

can be set in Cell 'H75' for automatic calculation of the chainage. The total length of remaining debris before overflowing the barrier (192 m) is entered to Cell 'D69'.

- (c) Volume of debris overflowing from barrier - a value of $2,520 \text{ m}^3$ ($= 3,300 \text{ m}^3 - 780 \text{ m}^3$) is entered into Cell 'D70' for this example.
- (d) Total length of debris chain - a 'rectangular' debris is assumed, and 'Landslide Mass Generator' can be used to produce a preliminary estimate of debris thickness. User can then modify the thickness of debris in Cells 'D74' to 'D84'. The debris thicknesses of the first two blocks (i.e. Block Nos. 10 and 11) are assigned to be 3.2 m (the maximum thickness of the remaining debris). The thickness is set to tail off towards the debris end to make up the remaining landslide volume of $2,520 \text{ m}^3$.

Figure B8 shows the input parameters for the debris mobility analysis. The spreadsheet is divided into several sections:

- 4. Interface Properties:**
 - Flow resistance on side slopes considered? (Yes = 1, No = 0)
 - Distance x for change from Interface (1) to (2) = 700 m
 - Interface (1) properties: Cohesion (c = 0 kPa), Friction angle (ϕ = 0°), Pore pressure ratio (r_u = 0), Turbulence coefficient (ξ = 300 m/s^2).
 - Interface (2) properties: Cohesion (c = 0 kPa), Friction angle (ϕ = 0°), Pore pressure ratio (r_u = 0), Turbulence coefficient (ξ = 0 m/s^2).
 - Entrainment/Deposition (Zone 1): Zone 1 starts at x = 40 m, Zone 1 ends at x = 65 m, Entrainment/deposition rate = 0.00 m^3/sec (-ve entrainment).
 - Entrainment/Deposition (Zone 2): Zone 2 starts at x = 65 m, Zone 2 ends at x = 330 m, Entrainment/deposition rate = -31.00 m^3/sec (-ve entrainment; +ve deposition).
 - Threshold Depth of Debris for Entrainment = 0.3 m, Min. Depth of Debris for Deposition = 0.3 m.
 - Consider Consolidation? (Yes = 1, No = 0, if 0 goto Row 68)
 - Fraction of Saturated Layer h_s = 0.1 (proportion of debris height, < 1)
 - Coefficient of Consolidation c_v = 6.3420E-05 m^2/s
- 5. Landslide Mass:**
 - Total Length of the Landslide Mass at Source = 192.0 m (for Landslide Mass Generator)
 - Total Volume of the Landslide Mass at Source = 2520 m^3 (for Landslide Mass Generator)
 - Initial debris velocity = 10.4 m/s
- 6. Analysis Parameters:**
 - Analysis stops at t = 200 s
 - Time step interval Δt = 0.01 s
 - Magnification factor for displaying the debris thickness = 10
 - No. of time steps between updating display and output = 50
- Landslide Mass Generator:**
 - Location, x of Block No. 10 = 173.0 m
 - Parabolic or Rectangular (P.R.)? r (for Landslide Mass Generator)
- Input the initial conditions of the landslide mass:**

Boundary block No.	Location, x (m)	Thickness, h (m)
1	173.0000	0.6000
2	186.4400	0.8200
3	201.8000	1.1000
4	221.0000	1.2500
5	240.2000	1.5000
6	269.0000	1.7000
7	297.8000	2.0000
8	317.0000	2.4000
9	336.2000	2.8000
10	351.3600	3.2000
11	365.0000	3.4000
Volume of landslide mass (m^3)		2520

Note: Parameters for Interface 2 is adopted for $x > 700 \text{ m}$ (see Row 51) but the total runout distance in the analysis is 525 m only, therefore, input to the flow resistance parameters for Interface 2 is irrelevant.

Figure B8 Input of Parameters which Govern the Initial Conditions of Debris Motion (Example No. 2)

The program 2d-DMM (version 1.2) takes into account the specified initial conditions to carry out debris mobility analysis. Hydrograph at the location of the second barrier B2 ($x = 460 \text{ m}$) can be obtained. Based on the hydrograph data and Kwan (2012), the design debris impact velocity is 7.3 m/s and the design debris thickness is 1.7 m (this combination

gives the maximum impact load). The corresponding design impact load is 408 kN/m ($\approx 2.5 \times 1,800 \times 7.3^2 / 1,000 \times 1.7$).

The procedures for calculating the design impact velocity and design debris thickness for the terminal barrier at $x = 525$ m are illustrated below.

Step (i) - carry out debris mobility analysis using a program prior accepted by GEO (e.g. 2d-DMM or DAN-W) to simulate the mobility of debris flow travelling from the landslide source to the first barrier.

Sheet 'Results for Post-processing' provides detailed output results for case of debris reaching the second barrier B2, which indicate that at $t = 9$ seconds the frontal debris mass block (i.e. Block 11) reaches $x = 460$ m (see part-print of Sheet 'Results for Post-processing' in Figure B9). The three front mass blocks (i.e. Blocks 9 to 11) constitute a volume of 950 m^3 , which is larger than the retention capacity of barrier at $x = 460$ m. Therefore, Blocks 9 to 11 and a portion of Block 9 will be retained by the barrier. The remaining volume is $2,520 \text{ m}^3$ minus 710 m^3 (retention volume of B2), which is equal to $1,810 \text{ m}^3$. This is a second analysis (from Barrier 1 to Barrier 2).

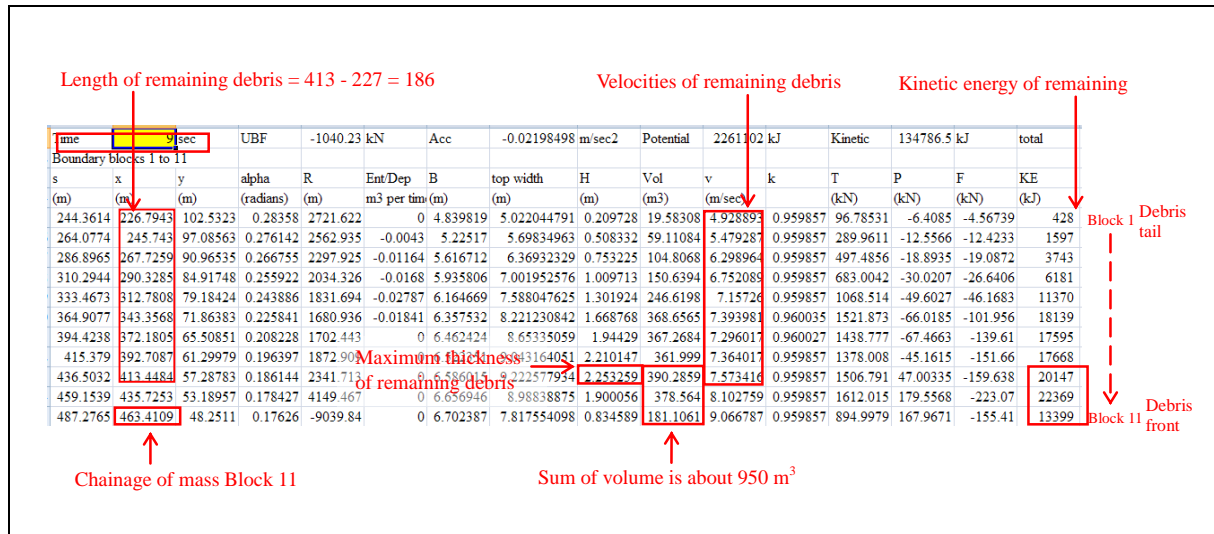


Figure B9 Output of 2d-DMM for the Second Intermediate Barrier (Example No. 2)

Step (ii) - use the results of the mobility analysis to determine the velocity at which debris will launch into a ballistic flight from the crest of the barrier.

The maximum velocity of the remaining debris would be taken as v_m for calculation of the length of debris trajectory (x_i). According to the calculation of the program 2d-DMM, the maximum velocity is 7.4 m/s.

Step (iii) - calculate geometry of the ballistic flight path and the debris velocity after landing.

With $v_m = 7.4$ m/s and channel inclination $\theta = 14^\circ$, and barrier height $h = 3$ m, a value of $x_i = 8$ m is obtained by using Equation 3.1. The barrier spacing between B2 and terminal

barrier at chainage $x = 525$ m in this example is 60 m, which is larger than both the length of projectile (8 m) and the minimum spacing calculated using the formula given in Figure 2.1, which is 41 m.

The kinetic energy (KE) of the debris that would not be trapped by the barriers can be calculated as follows (KE of each mass block can be found in Column 'P' of the output sheet, see also Figure B9):

KE of Block 1	=	428 kJ
KE of Block 2	=	1,597 kJ
KE of Block 3	=	3,743 kJ
KE of Block 4	=	6,181 kJ
KE of Block 5	=	11,370 kJ
KE of Block 6	=	18,139 kJ
KE of Block 7	=	17,595 kJ
KE of Block 8	=	17,668 kJ
Sub-total	=	76,721 kJ
KE from Block 9	=	12,398 kJ

Total = 89,119 kJ

Volume of this block = 390 m³
 Volume of debris that cannot be trapped
 by barrier = 240 m³
 Total KE of Block 9 = 20,147 kJ
 \therefore KE of the volume escaped
 = 20,147 x 240/390
 = 12,398 kJ

It follows that the KE of the remaining debris (KE_r) i.e. that cannot be retained by the barrier is 89,119 kJ. The remaining debris mass $m_r = (2,520 - 710) \text{ m}^3 \times 1,800 \text{ kg/m}^3 = 3,258,000 \text{ kg}$. Using Equations 3.2 and 3.3, the debris velocities at landing (v_r) and after landing (v_i) are calculated to be 11.9 m/s and 6.6 m/s respectively, by assuming the value of $R = 0.7$, $C_r = 1.0$ and $C_x = 0.8$. (Designers should note that use of a larger value of R may be warranted in design; C_x value is determined from Table 3.1 based on the ratio of the rear velocity to frontal velocity of the remaining debris ($4.9/7.5 = 0.65$), see Figure B9.)

Step (iv) - carry out debris mobility analysis to model debris flow travelling from the landing position to the next barrier.

The frontal thickness of debris at landing (h_m) is assumed to be the maximum thickness of the remaining debris (Block 1 to Block 9) before overflowing from the barrier. From the output shown in Figure B9, h_m is 2.2 m and the total length of the landslide mass is assumed to be the length of remaining debris before overflowing from the barrier. The following parameters are specified for the mobility analysis:

- Initial debris velocity - this is the debris velocity in the direction of the fall of the drainage line, it should be input to Cell 'D71' on Sheet 'Input' of 2d-DMM (see also Figure B10). In this example, the initial velocity is 6.6 m/s.
- Initial location of Block 1 - this is the chainage of the rear end of the debris chain and is input to Cell 'H75'. This chainage relates to the location of the barrier (i.e. $x = 460$ m), the length of trajectory (i.e. 8 m) and the total length of the debris chain (in Cell 'D69'). Formula " $= 460 + 8 - D69$ "

can be set in Cell 'H75' for automatic calculation of the chainage. The total length of remaining debris before overflowing the barrier (186 m), which is input to 'D69'.

- (c) Volume of debris overflowing from barrier - a value of $1,810 \text{ m}^3$ ($= 2,520 \text{ m}^3 - 710 \text{ m}^3$) is entered into Cell 'D70'.
- (d) Total length of debris chain - a 'rectangular' debris is assumed, and 'Landslide Mass Generator' can be used to produce a preliminary estimate of debris thickness. User can then modify the thickness of debris in Cells 'D74' to 'D84'. The debris thicknesses of the first two blocks (i.e. Block Nos. 10 and 11) are assigned to be 2.2 m (the maximum thickness of the remaining debris). The thickness is specified to tail off towards the debris end to make up the remaining landslide volume of $1,810 \text{ m}^3$.

47

48 **4. Interface Properties**

49 Flow resistance on side slopes considered? 1 (Yes = 1, No = 0)

50 (The above is only applicable when trapezoidal channel section module is used)

51 Distance x for change from Interface (1) to (2) = 700 m

52

53 Interface (1)

54 Cohesion c = 0 kPa

55 Friction angle $\phi = 8^\circ$

56 Pore pressure ratio $r_u = 0$

57 Turbulence coefficient $\xi = 500 \text{ m/s}^2$

58

59 Entrainment/Deposition (Zone 1)

60 Zone 1 starts at x = 40 m

61 Zone 1 ends at x = 65 m

62 Entrainment/deposition rate = 0.00 m^3/sec (-ve entrainment)

63

64 Threshold Depth of Debris for Entrainment = 0.5 m

65 Min. Depth of Debris for Deposition = 0 m

66

67

68 **5. Landslide Mass**

69 Total Length of the Landslide Mass at Source = 186.0 m (for Landslide Mass Generator)

70 Total Volume of the Landslide Mass at Source = 1810 m^3 (for Landslide Mass Generator)

71 Initial debris velocity = 6.6 m/s

72 Input the initial conditions of the landslide mass:

73 Boundary block No. Location, x (m) Thickness, h (m)

74 1 282.0000 0.3000

75 2 295.0200 0.4600

76 3 309.9000 0.6600

77 4 328.5000 0.8600

78 5 347.1000 1.0500

79 6 375.0000 1.2200

80 7 402.9000 1.5000

81 8 421.5000 1.7000

82 9 440.1000 2.0000

83 10 454.9800 2.2000

84 11 468.0000 2.2000

85 Volume of landslide mass (m^3) = 1810

86

87 **Start Analysis**

88

89

Interface (2)

Cohesion c = 0 kPa

Friction angle $\phi = 0^\circ$

Pore pressure ratio $r_u = 0$

Turbulence coefficient $\xi = 0 \text{ m/s}^2$

Entrainment/Deposition (Zone 2)

Zone 2 starts at x = 65 m

Zone 2 ends at x = 330 m

Entrainment/deposition rate = -31.00 m^3/sec (-ve entrainment; -ve deposition)

Consider Consolidation? 0 (Yes = 1, No = 0, if 0 goto Row 68)

Fraction of Saturated Layer $h_s = 0.1$ (proportion of debris height, < 1)

Coefficient of Consolidation $c_v = 6.3420E-05 \text{ m}^2/\text{s}$

6. Analysis Parameters

Analysis stops at t = 200 s

Time step interval $\Delta t = 0.01 \text{ s}$

Magnification factor for displaying the debris thickness = 10

No. of time steps between updating display and output = 50

Landslide Mass Generator

Location, x of Block No. 11 = 468.0 m

Parabolic or Rectangular (P/R)? r (for Landslide Mass Generator)

Note: Parameters for Interface 2 is adopted for $x > 700 \text{ m}$ (see Row 51) but the total runout distance in the analysis is 525 m only, therefore, input to the flow resistance parameters for Interface 2 is irrelevant.

Figure B10 Input of Parameters which Govern the Initial Conditions of Debris Motion for the Second Intermediate Barrier (Example No. 2)

The program 2d-DMM (version 1.2) takes into account the specified initial conditions to carry out debris mobility analysis. The analysis shows that the debris reaches the terminal barrier at $x = 525 \text{ m}$ at a design debris velocity of 7.5 m/s and the corresponding debris thickness is 1.0 m (c.f. velocity = 7.8 m/s and debris thickness = 2.1 m when a single barrier is

used) based on the maximum impact load derived from the combination of debris velocity and thickness. The corresponding design impact load is 253 kN/m ($\approx 2.5 \times 1,800 \times 7.5^2/1,000 \times 1.0$). This is about 56% less than that in the case of the single barrier design.

B.3.1 Discussion on Example No. 2

The result of using three barriers in this example shows that the design debris impact velocity at the terminal barrier is similar to the original single barrier scheme. However, the debris thickness is reduced notably from 2.1 m to 1.0 m. Also, the design impact velocity at the location of barrier B2 is less than the original case without any intermediate barriers (see comparisons given in Table B1). This results in the reduction of design impact load by some 40% to 50% and probably savings in the construction cost.

Table B1 Comparison of Numerical Results for Single Barrier and Multiple Barriers

Chainage	Design Impact Load (kN/m)	
	No Multiple Barrier	With Multiple Barriers
Ch 350	1,610	1,610
Ch 460	680	408
Ch 525	575	253

(a) Design Impact Load

Chainage	Design Impact Velocity (m/s)		Design Debris Thickness (m)	
	No Multiple Barrier	With Multiple Barriers	No Multiple Barrier	With Multiple Barriers
Ch 350	11.3	11.3	2.8	2.8
Ch 460	8.3	7.3	2.2	1.7
Ch 525	7.8	7.5	2.1	1.0

(b) Design Impact Velocity and Thickness

B.4 Reference

Kwan, J.S.H. (2012). *Supplementary Technical Guidance on Design of Rigid Debris-resisting Barriers (Technical Note No. TN 2/2012)*. Geotechnical Engineering Office, Hong Kong, 85 p.

GEO PUBLICATIONS AND ORDERING INFORMATION

土力工程處刊物及訂購資料

A selected list of major GEO publications is given in the next page. An up-to-date full list of GEO publications can be found at the CEDD Website <http://www.cedd.gov.hk> on the Internet under "Publications". Abstracts for the documents can also be found at the same website. Technical Guidance Notes are published on the CEDD Website from time to time to provide updates to GEO publications prior to their next revision.

Copies of GEO publications (except geological maps and other publications which are free of charge) can be purchased either by:

Writing to
Publications Sales Unit,
Information Services Department,
Room 626, 6th Floor,
North Point Government Offices,
333 Java Road, North Point, Hong Kong.

or

- Calling the Publications Sales Section of Information Services Department (ISD) at (852) 2537 1910
- Visiting the online Government Bookstore at <http://www.bookstore.gov.hk>
- Downloading the order form from the ISD website at <http://www.isd.gov.hk> and submitting the order online or by fax to (852) 2523 7195
- Placing order with ISD by e-mail at puborder@isd.gov.hk

1:100 000, 1:20 000 and 1:5 000 geological maps can be purchased from:

Map Publications Centre/HK,
Survey & Mapping Office, Lands Department,
23th Floor, North Point Government Offices,
333 Java Road, North Point, Hong Kong.
Tel: (852) 2231 3187
Fax: (852) 2116 0774

Requests for copies of Geological Survey Sheet Reports and other publications which are free of charge should be directed to:

For Geological Survey Sheet Reports which are free of charge:

Chief Geotechnical Engineer/Planning,
(Attn: Hong Kong Geological Survey Section)
Geotechnical Engineering Office,
Civil Engineering and Development Department,
Civil Engineering and Development Building,
101 Princess Margaret Road,
Homantin, Kowloon, Hong Kong.
Tel: (852) 2762 5380
Fax: (852) 2714 0247
E-mail: jsjewell@cedd.gov.hk

For other publications which are free of charge:

Chief Geotechnical Engineer/Standards and Testing,
Geotechnical Engineering Office,
Civil Engineering and Development Department,
Civil Engineering and Development Building,
101 Princess Margaret Road,
Homantin, Kowloon, Hong Kong.
Tel: (852) 2762 5346
Fax: (852) 2714 0275
E-mail: florenceko@cedd.gov.hk

部份土力工程處的主要刊物目錄刊載於下頁。而詳盡及最新的土力工程處刊物目錄，則登載於土木工程拓展署的互聯網網頁 <http://www.cedd.gov.hk> 的“刊物”版面之內。刊物的摘要及更新刊物內容的工程技術指引，亦可在這個網址找到。

讀者可採用以下方法購買土力工程處刊物(地質圖及免費刊物除外):

書面訂購
香港北角渣華道333號
北角政府合署6樓626室
政府新聞處
刊物銷售組

或

- 致電政府新聞處刊物銷售小組訂購 (電話: (852) 2537 1910)
- 進入網上「政府書店」選購，網址為 <http://www.bookstore.gov.hk>
- 透過政府新聞處的網站 (<http://www.isd.gov.hk>) 於網上遞交訂購表格，或將表格傳真至刊物銷售小組 (傳真: (852) 2523 7195)
- 以電郵方式訂購 (電郵地址: puborder@isd.gov.hk)

讀者可於下列地點購買1:100 000、1:20 000及1:5 000地質圖：

香港北角渣華道333號
北角政府合署23樓
地政總署測繪處
電話: (852) 2231 3187
傳真: (852) 2116 0774

如欲索取地質調查報告及其他免費刊物，請致函：

免費地質調查報告:

香港九龍何文田公主道101號
土木工程拓展署大樓
土木工程拓展署
土力工程處
規劃部總土力工程師
(請交:香港地質調查組)
電話: (852) 2762 5380
傳真: (852) 2714 0247
電子郵件: jsjewell@cedd.gov.hk

其他免費刊物:

香港九龍何文田公主道101號
土木工程拓展署大樓
土木工程拓展署
土力工程處
標準及測試部總土力工程師
電話: (852) 2762 5346
傳真: (852) 2714 0275
電子郵件: florenceko@cedd.gov.hk

MAJOR GEOTECHNICAL ENGINEERING OFFICE PUBLICATIONS

土力工程處之主要刊物

GEOTECHNICAL MANUALS

Geotechnical Manual for Slopes, 2nd Edition (1984), 302 p. (English Version), (Reprinted, 2011).

斜坡岩土工程手冊(1998) , 308頁(1984年英文版的中文譯本)。

Highway Slope Manual (2000), 114 p.

GEOGUIDES

Geoguide 1 Guide to Retaining Wall Design, 2nd Edition (1993), 258 p. (Reprinted, 2007).

Geoguide 2 Guide to Site Investigation (1987), 359 p. (Reprinted, 2000).

Geoguide 3 Guide to Rock and Soil Descriptions (1988), 186 p. (Reprinted, 2000).

Geoguide 4 Guide to Cavern Engineering (1992), 148 p. (Reprinted, 1998).

Geoguide 5 Guide to Slope Maintenance, 3rd Edition (2003), 132 p. (English Version).

岩土指南第五冊 斜坡維修指南，第三版(2003) , 120頁(中文版)。

Geoguide 6 Guide to Reinforced Fill Structure and Slope Design (2002), 236 p.

Geoguide 7 Guide to Soil Nail Design and Construction (2008), 97 p.

GEOSPECS

Geospec 1 Model Specification for Prestressed Ground Anchors, 2nd Edition (1989), 164 p. (Reprinted, 1997).

Geospec 3 Model Specification for Soil Testing (2001), 340 p.

GEO PUBLICATIONS

GCO Publication Review of Design Methods for Excavations (1990), 187 p. (Reprinted, 2002).
No. 1/90

GEO Publication Review of Granular and Geotextile Filters (1993), 141 p.
No. 1/93

GEO Publication Foundation Design and Construction (2006), 376 p.
No. 1/2006

GEO Publication Engineering Geological Practice in Hong Kong (2007), 278 p.
No. 1/2007

GEO Publication Prescriptive Measures for Man-Made Slopes and Retaining Walls (2009), 76 p.
No. 1/2009

GEO Publication Technical Guidelines on Landscape Treatment for Slopes (2011), 217 p.
No. 1/2011

GEOLOGICAL PUBLICATIONS

The Quaternary Geology of Hong Kong, by J.A. Fyfe, R. Shaw, S.D.G. Campbell, K.W. Lai & P.A. Kirk (2000), 210 p. plus 6 maps.

The Pre-Quaternary Geology of Hong Kong, by R.J. Sewell, S.D.G. Campbell, C.J.N. Fletcher, K.W. Lai & P.A. Kirk (2000), 181 p. plus 4 maps.

TECHNICAL GUIDANCE NOTES

TGN 1 Technical Guidance Documents